United States
Environmental Protection
Agency

Office of Research and
Development
Washington DC 20460

EPA/600/R-01/007a
March 2001

Multispecies Reactive Tracer Test in a Sand and Gravel Aquifer, Cape Cod, Massachusetts

Part 1

Experimental Design and Transport of Bromide and Nickel-EDTA Tracers

EPA/600/R-01/007a
March 2001

Multispecies Reactive Tracer Test in a Sand and Gravel Aquifer, Cape Cod, Massachusetts

Part 1
Experimental Design and Transport of Bromide and Nickel-EDTA Tracers

J. A. Davis[1], K. M. Hess[2], J. A. Coston[1], D. B. Kent[1], J. L. Joye[1], P. Brienen[1] and K. W. Campo[2]

[1] U.S. Geological Survey
Menlo Park, CA 94025

[2] U.S. Geological Survey
Northborough, MA 01532

Interagency Agreement DW14935626

Project Officer
Robert W. Puls
Subsurface Protection and Remediation Division
National Risk Management Research Laboratory
Ada, OK 74820

National Risk Management Research Laboratory
Office of Research and Development
U.S. Environmental Protection Agency
Cincinnati, OH 45268

Notice

The U. S. Environmental Protection Agency through its Office of Research and Development partially funded and collaborated in the research described here under Interagency Agreement DW14935626. It has been subjected to the Agency's peer and administrative review and has been approved for publication as an EPA document. Mention of trade names or commercial products does not constitute endorsement or recommendation for use.

All research projects making conclusions or recommendations based on environmentally related measurements and funded by the Environmental Protection Agency are required to participate in the Agency Quality Assurance Program. This project was conducted under an approved Quality Assurance Project Plan. The procedures specified in this plan were used without exception. Information on the plan and documentation of the quality assurance activities and results are available from the Principal Investigator.

Foreword

The U.S. Environmental Protection Agency is charged by Congress with protecting the Nation's land, air, and water resources. Under a mandate of national environmental laws, the Agency strives to formulate and implement actions leading to a compatible balance between human activities and the ability of natural systems to support and nurture life. To meet this mandate, EPA's research program is providing data and technical support for solving environmental problems today and building a science knowledge base necessary to manage our ecological resources wisely, understand how pollutants affect our health, and prevent or reduce environmental risks in the future.

The National Risk Management Research Laboratory (NRMRL) is the Agency's center for investigation of technological and management approaches for preventing and reducing risks from pollution that threatens human health and the environment. The focus of the Laboratory's research program is on methods and their cost-effectiveness for prevention and control of pollution to air, land, water, and subsurface resources; protection of water quality in public water systems; remediation of contaminated sites, sediments and ground water; prevention and control of indoor air pollution; and restoration of ecosystems. NRMRL collaborates with both public and private sector partners to foster technologies that reduce the cost of compliance and to anticipate emerging problems. NRMRL's research provides solutions to environmental problems by: developing and promoting technologies that protect and improve the environment; advancing scientific and engineering information to support regulatory and policy decisions; and providing the technical support and information transfer to ensure implementation of environmental regulations and strategies at the national, state, and community levels.

The use of multispecies reactive transport modeling in site assessments and remedial performance monitoring at hazardous waste sites is to be encouraged. These can be valuable tools for simulating processes which govern contaminant fate and transport in the subsurface. A competent reactive transport model of a site must be able to simulate the processes that occur between water and the vapor and solid phases in contact with the water. The accuracy of such simulations will be dependent on the database contained within such models as well as the quality of the site-specific data collection efforts.

The lessons learned from the large-scale tracer tests and subsequent modeling investigations from this study have implications that go far beyond the particular contaminant species studied here. For homogeneous and classical heterogeneous reactions (e.g., dissolution equilibria), there are generally available equilibrium constants that may be used with confidence in such models; however, solubilities for poorly crystalline or impure solid phases are generally not available and will have to be determined using site-specific materials. Adsorption and other heterogeneous surface reactions will generally require experimental determination of parameters that are site-specific. In addition, chemical reactions can be rate-limited and controlled by physical factors such as diffusion or mixing of waters across sediment layers. These studies were important in identifying the limitations of reactive transport modeling, their utility, and where additional data collection and testing is warranted.

Stephen G. Schmelling, Acting Director
Subsurface Protection and Remediation Division
National Risk Management Research Laboratory

Executive Summary

Constructing an accurate and predictive mathematical simulation of reactive transport of metal ions in groundwater requires detailed knowledge about metal ion solubility and sorption under the local geochemical conditions of the aquifer. While distribution coefficients may be sufficient to describe sorption for simulations under constant chemical conditions, the surface complexation model approach is better suited when chemical conditions vary. However, both approaches suffer from a lack of datasets collected under aquifer-scale temporal and spatial dimensions.

A comprehensive field investigation of multispecies reactive transport under variable chemical conditions was conducted in a shallow, unconfined sand and gravel aquifer on Cape Cod, Massachusetts. Nearly ten thousand liters of groundwater with additional tracers were injected into the aquifer. The distribution of tracers was monitored for over a year as the tracers were transported over 200 meters through an array of multilevel samplers. The added tracers were comprised of a nonreactive solute Br (bromide ion) and the reactive solutes Cr(VI) (chromium in the plus six oxidation state), and EDTA (ethylenediaminetetraacetic acid) complexes of four divalent metal cations: Cu (copper), Ni (nickel), Pb (lead), and Zn (zinc). A small excess of EDTA was added to ensure that the speciation of the metal ions was dominated by anionic EDTA complexes. Transport was quantified using spatial moments compiled from comprehensive synoptic samplings of the tracer cloud and temporal moments (breakthrough curves) of concentration data collected at two MLS.

Variable geochemical conditions in the aquifer resulted from the presence of a plume of sewage-contaminated groundwater overlain by pristine recharge groundwater. The pristine zone had high dissolved oxygen concentrations, pH values in the range of 5.4 to 5.7 and low dissolved salt concentrations. The sewage-contaminated zone was suboxic and mildly reducing with DO (dissolved oxygen) concentrations less than 3 micromolar and pH values in the range of 6.0- to 6.5, and increased dissolved salt concentrations including sewage-derived contaminants such as phosphate and borate. Gradients in dissolved solutes were present between the pristine and sewage-contaminated zones over an approximately 2.5 meter thick interval. A portion of the sewage-contaminated zone near the upper boundary had elevated concentrations of both dissolved and adsorbed Zn. The tracers were injected over a vertical interval that spanned all the geochemical conditions (pristine, Zn-contaminated, and sewage-contaminated zones). Injection of the tracers into the aquifer resulted in some minor changes in aquifer chemistry, but these changes had little influence on the transport of reactive tracers after the first few weeks of the experiment.

The spatial extent of the distribution of Br increased over time, due to the physical processes of dispersion and sinking caused by the density difference between the tracer cloud and the ambient groundwater. The greatest dispersion was observed in the direction of flow. Bromide traveled a slightly curved path, caused by a change in the direction of groundwater flow during the test.

Metal exchange reactions, in which the metal ion of one of the injected metal-EDTA complexes was displaced by another cation such as Fe, Al or Zn, were expected to affect the distribution of the injected metal-EDTA tracers. Little or no metal exchange with the Ni-EDTA complexes occurred during the test. Although there was an initial loss of dissolved Ni mass from the cloud (by about 14%), Ni-EDTA transport was nearly conservative during the tracer test. The loss was attributed to reversible adsorption of the Ni-EDTA complex onto the aquifer solids and not to exchange reactions. A similar trend was found for EDTA (as the total of all the complexes present).

Ni-EDTA was retarded the least of the injected tracers (the average retardation factor was 1.2). Adsorption of anionic solutes was favored under the lower pH and dissolved salt concentrations characteristic of the pristine zone in this aquifer. Retardation factors (R_f) calculated from temporal samplings conducted in the different aquifer zones showed that Ni-EDTA was indeed more strongly retarded under pristine zone conditions relative to bromide (R_f = 2.07).

Contents

Tables

Figures

Abbreviations

d	Day
DO	dissolved oxygen
EDTA	ethylenediaminetetraacetic acid
g	Grams
ICP-AES	inductively-coupled plasma atomic emission spectroscopy
kg	Kilograms
km	Kilometers
L	Liters
m	Meter
µg	Micrograms
µM	Micromoles per liter
mg	Milligrams
mM	Millimoles per liter
mm	Millimeters
M	Moles
MLS	multilevel sampler
nm	Nanometers
QC	quality control

SI Conversion Factors

Multiply	English (US) Units	by	Factor	to get	Metric (SI) Units
Area:	1 ft^2		0.0929		m^2
	1 in^2		6.452		cm^2
Flow rate:	1 gal/min		6.31×10^{-5}		m^3/s
	1 gal/min		0.0631		L/s
	1 MGD		43.81		L/s
Length:	1 ft		0.3048		m
	1 in		2.54		cm
Mass:	1 lb		453.59		g
	1 lb		0.45359		kg
Volume:	1 ft^3		28.316		L
	1 ft^3		0.028317		m^3
	1 gal		3.785		L
	1 gal		0.003785		m^3
Temperature:	^oF - 32		0.55556		^oC
Concentration:	1 gr/ft^3		2.2884		g/m^3
	1 gr/gal		0.0171		g/L
	1 lb/ft^3		16.03		g/L
Pressure:	1 lb/in^2		0.07031		kg/cm^2
	1 lb/in^2		6894.8		Newton/m^2
Heating value:	Btu/lb		2326		Joules/kg
	Btu/scf		37260		Joules/scm

Acknowledgments

We are grateful to Drs. B. Bekins, J. Friedly, and J. Zobrist for critical technical reviews of the report. Numerous people contributed to the field and laboratory work reported here. Technical and field assistance were provided by S. Coppola, W. Carothers, G. Granato, M. Kohler, M. Kruger, J. Masterson, T. McCobb, B. Mitch, B. Rea-Kumler, and J. Savoie, sometimes under unfavorable conditions. C. Ogle (Ogle Tooling) and M. Fitzgerald (Design Craft Woodworks) provided critical assistance in the design and construction of the apparatus used for processing "Chelex" samples. S. Wallace conducted laboratory experiments on chemical interactions between EDTA and aquifer sediments described in the text. C. Fuller and L. Anderson provided technical advice on experimental design, sampling, and analysis at various stages during the project. The numerous contributions of Denis LeBlanc, USGS Cape Cod Groundwater Research Site Coordinator, and Dr. Robert Puls, Project Officer, Subsurface Protection and Remediation Division, National Risk Management Research Laboratory, Office of Research and Development, U.S. Environmental Protection Agency, are gratefully acknowledged. Funding for the project was provided by the U.S. Environmental Protection Agency, Office of Research and Development, through interagency agreement number DW14935626 and the U.S. Geological Survey Toxic Substances Hydrology Program.

Introduction

In the past decade many reactive transport models have been developed to describe the effects of chemical reactions on the transport of solutes (e.g., Liu and Narasimhan, 1989; Yeh and Tripathi, 1991; Parkhurst, 1995; Curtis and Rubin, submitted). The reactivity of inorganic solutes depends strongly on chemical speciation; species that precipitate or are extensively adsorbed are highly retarded, whereas species that are soluble and weakly adsorbed can be mobile in groundwater (Davis et al., 1993). Much of the discussion about these models has been concerned with the most efficient mathematical coupling of transport equations (partial differential equations) with the algebraic equations that describe chemical reactions at equilibrium (e.g., see Yeh and Tripathi, 1989; and Rubin, 1990). Other issues of interest in model development have included: 1) the validity of the assumption of local chemical equilibrium, 2) the comprehensiveness of the models in terms of complex geochemical and hydrophysical processes (e.g., Yeh and Tripathi, 1989), and 3) the capability of treating a combination of mixed chemical equilibria and chemical rate expressions.

While it appears that considerable advances are being made in the development of mathematical algorithms, many practical problems remain if reactive transport models are to be applied to groundwater systems in predictive simulations. For example, adsorption reactions require special considerations. Some reactive transport models have relied on empirical parameters, such as distribution coefficients or isotherms determined in laboratory studies, to describe retardation of solutes during transport. While this approach may be satisfactory under constant chemical conditions, the surface complexation modeling approach will provide better results under conditions of variable chemistry (Kent et al., 2000a, Davis et al., 1998; Kohler et al., 1996; Davis and Kent, 1990). Adsorption is affected by competitive adsorption processes (Stollenwerk, 1995), solute speciation changes (Waite et al., 1994), and other factors under conditions of variable chemical conditions. In the surface complexation approach, adsorption is considered as a set of one or more chemical reactions involving an aqueous species, a surface site on the porous medium, and protons. In principle, reactions are required for each adsorbing solute, however, laboratory data may be used to minimize the number of reactions needed for a transport modeling application. Examples of reactive transport models that have used the surface complexation approach are those of Cederberg et al. (1985), Hostetler et al. (1989), Yeh and Tripathi (1991), Kohler et al. (1996), Stollenwerk (1998), and Kent et al. (2000a).

Despite recent developments in reactive transport modeling, the application of such models and computer codes to real-world problems is still limited by the lack of relevant kinetic and thermodynamic data for describing appropriate sorption and redox reactions in the environment. Further advances in this area will require the development of operating paradigms for field problems, perhaps including approaches for estimating a distribution of significant model parameters using site-specific materials. However, current experimental procedures with site-specific materials involve studies with short contact times (batch studies), small samples (less than a kilogram), and for column studies, short path lengths (less than one meter), as compared to the time and space dimensions of real systems. Questions remain concerning the applicability of chemical parameters determined in laboratory studies to model simulations of solute transport in large field studies.

In this report, we summarize a portion of the results of a large-scale tracer test conducted at the U. S. Geological Survey research site on Cape Cod, Massachusetts. The site is located on a large sand and gravel glacial outwash plain in an unconfined aquifer. In April 1993, about 10,000 liters of groundwater from the site were injected into the shallow aquifer with bromide (Br), chromate (Cr(VI)), and four metals (lead (Pb), copper (Cu), nickel (Ni), zinc (Zn)) complexed with ethylenediaminetetraacetic acid (EDTA) added as tracers. At the time of the tracer test, shallow groundwater at the site was contaminated by secondary sewage effluent that was discharged since 1936 onto infiltration beds located about 240 m (meters) upgradient of the injection wells. Vertical concentration gradients in dissolved oxygen, pH, dissolved Zn, and other water quality parameters are caused by the mixing of the sewage effluent with ambient groundwater (Kent et al., 1994). The experiment was carried out such that the water with tracers would be injected across these vertical gradients in water quality. Thus, the mobility of the tracers under variable chemical conditions could be compared and the fate of the tracers in response to different chemical processes could be contrasted. The main objectives of the experiment were:

1. to demonstrate the importance of chemical reactions, aqueous speciation, and variable background chemical conditions on the transport of selected toxic elements (Cr, Pb, Cu, Zn, Ni) in groundwater;
2. to compare the rates and extents of chemical reactions observed in a field study with those measured under similar conditions in laboratory experiments;
3. to examine the relationships between chemical and hydrologic processes in solute transport;
4. to examine the importance of the spatial variability of geochemical properties and its impact on reactive transport;
5. to investigate the problem of modeling flow coupled with chemical reactions in the groundwater environment with a view towards simplification of the geochemical reaction network;
6. to contribute a well-characterized but chemically complex data set to the literature that would spur the development and/or application of hydrogeochemical transport models of flow coupled with chemical reactions; and,
7. to examine the methods of parameter estimation used for describing reactive chemical processes during transport and to compare such parameters with those determined from laboratory, small-scale field, and modeling investigations.

This report discusses the experimental design and execution of the test and the quantitative description of bromide, EDTA, and nickel-EDTA transport during the test. Experimental results for the transport of the remaining tracers (Cr, Pb, Cu, and Zn) are presented in a companion report (Davis et al., 2000).

Site Description and Aquifer Characteristics

The tracer test was conducted in an abandoned gravel pit on western Cape Cod near the Massachusetts Military Reservation (MMR, also known as Otis Air Base, Figure 1) at the U.S. Geological Survey Toxic Substances Hydrology Research site. An earlier tracer test, designed primarily to study macrodispersion of solutes in the subsurface, was conducted at the site and demonstrated the suitability of the site to tests of this type (Garabedian et al., 1991; LeBlanc et al., 1991).

Hydrogeologic Characteristics

The site is located between the MMR sewage disposal beds and Ashumet Pond (Figure1). The unconsolidated sand and gravel deposits form an unconfined aquifer that serves as the sole source of drinking water in the area, as well as being the primary receptor of domestic, municipal, agricultural, and industrial wastes. The water table is 4 - 7 meters (m) below land surface and slopes to the south at 1.6 m per 1000 m (Figure 1). Fifty centimeters per year (cm/yr) of water, which is about 45% of the total annual precipitation, is estimated to recharge the ground-water system (LeBlanc et al., 1986). Most recharge occurs in the late fall and winter when evaporation and plant transpiration is minimal. Recharge occurs across the tracer test site, evidenced by the wedge of pristine water that accumulated over the tracer clouds in this test (see below) and the test previously conducted at the site (LeBlanc et al., 1991). On a larger scale, this accumulation of clean recharge water at the top of the aquifer can be seen over the sewage plume which underlies this site.

The aquifer is composed of about 100 m of unconsolidated sediments that overlie a relatively impermeable crystalline bedrock (Oldale, 1969). The upper 30 m of the aquifer, in which this experiment was conducted, consists of stratified sand and gravel outwash of glaciodeltaic origin (Masterson et al., 1997). This permeable unit has a median grain size (by weight) of about 0.5 mm, is moderately sorted, and contains less than 1% silt and clay sized fractions (Barber et al., 1992). The sediments are composed primarily of quartz (95%) with minor amounts of feldspar and ferromagnetic minerals (Barber et al., 1992; Coston et al., 1995). Most sediment grains have coatings of Fe and Al oxyhydroxides (Coston et al., 1995). The amount of organic carbon in the sediments is typically less than 0.01% by weight (Barber et al., 1992). Beneath the sand and gravel deposits the sediments consist of a fine-grained sand and silt deposit of glaciolacustrine origin (Masterson et al., 1997).

The estimated average horizontal hydraulic conductivity of the sand and gravel is 95 meters per day (m/d; Hess et al., 1992). This average was obtained from 825 hydraulic tests conducted with a flowmeter in 16 long-screened wells located within 50 m of the tracer-test site. The average hydraulic conductivity is similar to the 110 m/d estimated from a large-scale aquifer test conducted in the outwash 2.2 kilometers (km) south of the site (Garabedian, 1987); the aquifer test yielded a ratio of horizontal to vertical hydraulic conductivity of 2:1 to 5:1. The hydraulic-conductivity estimates from the flowmeter tests range over an order of magnitude. This variability results from the interbedded sand and gravel lenses that are evident in surface exposures of the outwash deposits (LeBlanc et al., 1991).

The effective porosity is estimated to be about 0.39 from the results of several small-scale tracer tests conducted within 2.5 km of this site (Garabedian, 1987; Barlow, 1987) and the large-scale tracer test previously conducted at this site (Garabedian et al., 1991). This estimated porosity is within the range of 0.36 to 0.42 reported by Perlmutter and Lieber (1970) and Morris and Johnson (1967) for sandy, stratified glacial deposits.

Despite the large amount of recharge, vertical hydraulic gradients are too small to measure in clusters of monitoring wells at the tracer-test site (LeBlanc et al., 1991). Groundwater flow is nearly horizontal. The average velocity of groundwater in the upper sand and gravel deposit is about 0.4 m/d based on the estimates of hydraulic gradient, hydraulic conductivity, and porosity given above.

Chemical Characteristics

Groundwater was contaminated by nearly 60 years (1936-1995) of discharge of secondarily-treated sewage effluent onto rapid infiltration sand beds located about 240 m upgradient of the study site. Effluent percolating through the unsaturated zone into the groundwater below created a plume of contaminated water that, by 1994, was greater than 5 km long (Savoie and LeBlanc, 1998). The contaminant plume (LeBlanc, 1984; Barber et al., 1988; Kent et al., 1994) contains elevated concentrations of dissolved inorganic solutes including calcium (Ca), magnesium (Mg), potassium (K), sodium (Na), sulfate, phosphate (PO_4), and boron (B). In addition, low concentrations of dissolved oxygen (DO), dissolved organic carbon (1-3 mg/L), and various detergent compounds are observed. Sewage-contaminated groundwater is slightly acidic to near-neutral (pH 5.8-6.9). Chemical conditions throughout most of the sewage-contaminated zone are mildly reducing, with concentrations of DO less than 35 micromoles per liter (μM), and variable concentrations of nitrate and manganese (Mn); concentrations of ferrous (Fe(II)) are below detection. This region of the sewage plume is referred to herein as the "suboxic zone." At a distance beginning about 180 m downgradient from the disposal beds (120 m upgradient of the injection site) the center of the sewage-contaminated region in the aquifer is anoxic at elevations between +7 and –4 m to sea level, with concentrations of Fe(II) up to 500 μM (Kent et al., 1994).

Vertical, longitudinal cross sections showing DO, pH, dissolved Mn, PO_4, Ca, Mg, Na, B, Si (dissolved silica), and Zn are presented in Figure 2. The horizontal axes of these sections show the distance downgradient of the injection multilevel samplers (MLS) used for this tracer test. Locations of the MLS used to construct the sections are given in Figure 3.

The plume is overlain by uncontaminated recharge water (referred to as pristine in this study), which has a lower pH (4.5-5.5), low concentrations of dissolved salts, and is saturated with DO (Kent et al., 1994). Dissolved B is extremely low in the uncontaminated groundwater and serves as a useful measure of the mixing of ambient groundwater with the secondary sewage effluent.

A small region of the aquifer is contaminated with Zn derived from sewage disposal. Zn and Cu are both present in the effluent discharged to the disposal beds (Vaccaro et al., 1979; Rea et al., 1991, 1996; Kent and Maeder, 1999). These metals are common constituents of domestic sewage effluents and are thought to be derived from corrosion of pipes in water distribution systems (Foerstner and van Lierde, 1983). Dissolved Zn concentrations were between 4-5 μM in the transition zone near the injection site (Figure 2). These concentrations of dissolved Zn are supported by Zn adsorbed to the aquifer sediments; concentrations of adsorbed Zn are approximately 100 times that of dissolved Zn (Davis et al., 1998). The region of Zn contamination thinned with distance downgradient, and the concentration of background dissolved Zn decreased to below detection at 165 m downgradient of the injection site (Figure 2). This point is the leading edge of the Zn being transported as a result of the sewage contamination (Kent et al., 2000a).

Definition of Geochemical Zones

In this report, for the purpose of discussing the influence of chemical conditions on the transport of tracers, we have defined zones of differing chemical conditions (Figure 4). Boron concentrations can be used to define two principal zones in the aquifer: the *pristine zone* (B below detection) and the *sewage-contaminated zone*. Steep vertical gradients in pH and the concentrations of DO, Zn, and other solutes occur at altitudes between 10 and 12.5 m to sea level (Figure 2). This region is referred to as the *transition zone*. The boundary between the *oxic zone* and *suboxic zone* is defined approximately by the 3 μM DO contour. Except for a few MLS located along the west side of the array, the anoxic zone at the center of the sewage contamination was located at elevations below the bottom ports of the MLS. None of the results presented in this report are from the anoxic zone of the aquifer. The region of the aquifer that had sewage-derived dissolved and adsorbed Zn is referred to as the *Zn-contaminated region*.

Design and Objectives of the Natural Gradient Injection

The injection was designed to take advantage of an existing array of MLS installed in the aquifer (LeBlanc et al., 1991). In the array, MLS are arranged in rows about 2 to 3 m apart that are aligned perpendicular to the average hydraulic gradient direction. There are 809 MLS in the array (Figure 3). Each MLS contains 15 sampling ports spaced vertically from 0.25 m to 0.76 m apart. Thus, chemical data can be collected at hundreds of precisely located points as tracers move downgradient of an injection site.

Six new MLS were installed for the injection in two closely-spaced rows of 3 MLS each (Figure 3) about 43 m downgradient of the injection location used by LeBlanc et al. (1991). The initial shape of the tracer cloud was intended to occupy a space 4 m wide (transverse horizontal direction, perpendicular to flow), 3 m in vertical thickness, and 2 m in depth (in the groundwater flow direction). Injectate water was pumped from a holding tank into three ports (at 13.17, 12.18, and 11.18 m elevation) of each of the six MLS, such that a significant portion of the injectate was injected into the pristine and sewage-contaminated zones of the aquifer.

The tracers were chosen based on their relative reactivities under the chemical conditions present at the field site. Adsorption of the injected anionic species was known to be pH dependent and a function of the concentration of competing anions from previous tracer tests (Kent et al., 1992, 1994, 1995, 2000b) and various laboratory studies (Bowers and Huang, 1986; Huang et al., 1988; Borggaard, 1991; Nowack and Sigg, 1996). Pb-, Cu-, Zn-, and Ni-EDTA complexes were chosen because of their relative stability constants (Martell and Smith, 1989) and calculated exchange order with respect to Fe oxyhydroxide dissolution by EDTA. Dissolution and metal exchange reactions with Fe- and aluminum (Al)-oxyhydroxides coating the aquifer sediments can occur with the metal-EDTA complexes. EDTA was chosen as a model ligand for metal complexation, because it was known to be resistant to biodegradation in the Cape Cod aquifer (Davis et al., 1993). Chromate transport was influenced by both adsorption and reduction of Cr(VI) to Cr(III), which is an immobile species. A previous tracer test at the site (Garabedian et al., 1991; LeBlanc et al., 1991) concluded that Br was a suitable choice for a nonreactive tracer.

EDTA was injected at a concentration in slight excess of the sum of concentrations for the four metals (Table 1). Speciation of Ni, Cu, Pb, and Zn was dominated by the complex, $MeEDTA^{2-}$, in the injectate water, where Me represents one of the four injected metal ions. Calculations based on available thermodynamic data (Smith and Martell, 1989) indicated that only minor amounts of other metal-EDTA complexes (e.g., $MeHEDTA^{-}$, $MeOHEDTA^{3-}$) were stable under the chemical conditions present in the injectate water or in the aquifer. To simplify the discussion, we shall use the general term of metal-EDTA complexes to refer to all of the complexes formed. Other than the metal-EDTA complexes, species of the four metals were below detection in the injected water.

Description of injection procedures

On April 20, 1993, nearly 10,000 liters of pristine groundwater were withdrawn from a well 400 m downgradient of the injection site and transported to an above-ground, plastic swimming pool installed at the site of the injection. At this well, the pristine zone was thicker than near the injection MLS making it easier to extract a sufficient volume of pristine groundwater for the experiment. It was confirmed that only pristine water was extracted by monitoring for changes in conductivity during pumping. All containers, including the swimming pool liner, were thoroughly cleaned with 0.01 moles per liter (M) EDTA and rinsed with deionized water before use. A concentrated solution of the EDTA and metal salts used in the test (Pb, Cu, Zn, Ni) was prepared twenty-four hours before the injection, to ensure that the metal-EDTA complexes were equilibrated. Cr(VI) and Br were added as salts to the holding tank on site after it was filled. The injectate solution was mixed with plastic paddles for 3 hours in the swimming pool. The water was injected into the aquifer through the 18 sampling ports of the 6 injection MLS at a rate of 1.02 liters/minute/port. The injection was accomplished over a nine-hour period on April 21, 1993. Small amounts of the tracers apparently entered the interior of the MLS during injection through the holes created for the sampling tubes, later exiting the MLS through its open bottom or through the same holes. This observation comes from the fact that low concentrations of tracers were detected at the bottommost port of the injection MLS 1 day after injection (Table 2). The mass of tracers that entered the interior of the injection MLS was small, but was not quantified. The filled circles in the MLS in Figure 2 at zero m downgradient show the sampling ports at which the tracers were detected 1 day after the injection. The vertical spreading of the initial injection extended from about 10 to >13.7 m elevation, spanning the chemical gradients as intended.

Periodically, throughout the injection, injectate was sampled for pH, EDTA, Br, and dissolved metals to check the homogeneity of the injected water. Differences in the tracer concentrations varied by less than 5% among these samples, demonstrating that the water in the holding tank was well mixed. The concentrations of the injected tracers and other details of the tracer injection are given in Table 1. The volume of the injected water and the tracer concentrations were chosen with the goal of observing measurable concentrations of the tracers for travel distances greater than 150 m and reactions times of one year or longer. Concentrations of Br and the metal tracers ranged from 500 to 4000 times their respective detection limits (Table 1).

Sample types

Three different types of water samples were collected during the field experiment described in this report: 1) anion, 2) cation, and 3) metal speciation. Each MLS port was purged of standing water prior to sampling. Anion samples were collected first, followed by the cation, and metal speciation samples. All samples were preserved immediately after collection. Table 3 summarizes the preservation treatments used (indicated in procedural order), the type of data collected, and the analytical method used. All wastewater was collected and sampled prior to disposal off-site. Assays of these “waste” samples were used to correct the calculated mass balances for the tracers. Additional information on sample collection and analyses is given in previously published reports (Davis et al., 1993; Kent et al., 1994, 1995).

Cation samples for total dissolved metals analyses were filtered inline with 0.45 μm (micrometers) PVDF (Millipore, Millex-HV, 25 millimeter diameter) syringe cartridge filters (use of brand names is for identification purposes only and does not imply endorsement by the USGS). Sample bottles were capped at all times except during filtration and acidification, to avoid contamination.

Metal speciation samples were filtered like cation samples, then passed through cartridges packed with Chelex-100 cation-exchange resin (Alltech cartridge columns or Bio-Rex ion exchange membranes) before acidification. The ion exchange membranes had the resin beads permanently mounted in a PTFE membrane (0.45 μm mesh). The resin bead size in the columns was 150 - 300 microns. The column resin contained charged functional groups (iminodiacetic acid) bound covalently to the insoluble column support. Mobile counterions, e.g., sodium (Na^+), were associated with the functional groups. When a sample is passed through the column, neutral and negatively charged ions pass through the column. Cations compete with the counterions for retention on the resin. Laboratory tests showed that the EDTA-complexed metals (Pb, Cu, Zn, Ni, Fe, Al, Mn) considered in the field experiment passed through the exchange column. Free metal ions were retained by the resin as long as the flow rate through the cartridge did not exceed 20 milliliters per minute. In this study, the measured difference in metal concentrations between cation and metal speciation samples at a given sampling location was defined as the free metal ion concentration. Of the four injected metals, significant free metal ion concentrations were only observed for Zn. Table 4 summarizes the analytical errors and limits of detection for the methods used in this study.

Sampling the tracer test

Two different sampling strategies were utilized during the tracer test: synoptic and breakthrough samplings. Synoptic samplings were conducted once per month during the period April to December 1993. The spatial extent of sampling was estimated based on the size and shape of the cloud from the previous sampling and checked in the field prior to beginning a synoptic sampling by measuring dissolved Br with the ion-specific electrode. Each synoptic sampling included MLS where the concentrations of the tracers were expected to be zero to ensure that the cloud boundaries were defined. Two additional synoptic samplings were conducted 314 and 449 days after the injection date to measure the amount of the reactive tracers remaining in the array and to determine whether background conditions had been re-established. Generally, only cation and anion sample types were collected during the synoptic sampling rounds (Table 2). Samples for metal speciation and pH measurements were also collected along two transects approximately parallel to the direction of flow (and the longest dimension of the tracer cloud) during most of the synoptic sampling rounds.

Breakthrough curves were collected from two MLS located 37 and 52 m downgradient from the injection site (Figure 3). Samples were collected a minimum of three days per week until all tracers were no longer detectable. Samples from both breakthrough MLS continued to be collected after the tracer cloud had passed to monitor the return to pre-test conditions. Metal speciation, pH, anion, and cation samples were collected for both MLS. All MLS were sampled with peristaltic pumps plumbed with silicon tubing using the sampling carts described in LeBlanc et al. (1991). Norprene tubing was used for the background measurements of DO.

Aqueous Chemistry Analyses

Field Site Measurements

The pH of anion water samples was measured in the field lab within 24 hours of collection and after samples had reached room temperature; the sample bottles were tightly capped between collection and pH measurement. pH was measured in static mode at a fixed equilibration time (3 minutes) and data recorded to 0.1 millivolts with a Ross combination electrode. All readings were recorded in millivolts and converted to pH using the mV readings of National Bureau of Standards traceable pH buffers. The buffers were measured before and after each set of 15 samples. The uncertainty in these measurements is probably due to variations in ionic strength and electrode drift.

Dissolved oxygen concentrations were measured using a membrane probe for concentrations above 30 μM as described in Kent et al. (1994). At lower concentrations DO was determined using the CHEMet method (Chemetrics Inc., Calverton, VA) described in Davis et al. (1993). A CHEMet is a glass ampule that contains a premeasured amount of Rhodazine D reagent sealed under vacuum. Changes in color intensity of the reagent indicate the amount of DO present.

EDTA concentrations were determined using the method of Bhattacharyya and Kunda (1971). In this method, sulfuric acid and an excess of Fe(III) over EDTA were added to each sample. Fe(III) displaced other metals from EDTA; the excess Fe(III) formed complexes with sulfate. The absorbance of each sample was measured at two different wavelengths in the UV range (258 and 305 nanometers (nm)) to distinguish between UV (ultra-violet) absorption by

Fe(III)-sulfate and Fe(III)-EDTA complexes. The absorbance measured at 258 nm was subtracted from that measured at 305 nm and this value was adjusted by the absorbance ratio (A258/A305) measured in a blank. The corrected absorbance value was used to calculate the concentration of EDTA in the sample using a standard curve. A linear concentration range was observed between 2-100 μM EDTA. Because the Fe(III)-EDTA complex is photosensitive, samples and standards were prepared and measured on the same day to minimize light exposure. A quality control (QC) sample of diluted composite injectate solution was measured every 10-15 samples. The detection limit and relative precision of EDTA measurements were much higher and lower, respectively, than the metals measurements, due to the presence of unknown, UV-absorbing constituents in the sewage-contaminated groundwater. All EDTA measurements were made within four days of collection.

Bromide Measurements

Bromide concentrations were estimated at the field site with an ion selective electrode. The linear range of this method in the Cape Cod groundwater was 0.125-6.26 mM (millimoles per liter). The field analyses were only used to estimate the location of the tracer cloud prior to sampling. More accurate and precise Br data were obtained using a colorimetric method (Franson, 1985) with a flow injection analyzer (Lachat Instruments). In this method, the sample is first pH-buffered and then Br is oxidized to BrOH (hypobromous acid) by hypochlorous acid. The BrOH reacts with fluoresceine dye, changing the color from green to pink (tetrabromofluorescein). The linear range of the method in standard solutions is 0.63-25.0 μM; however, the method limit of detection in undiluted Cape Cod groundwater was 3 μM. For the Br analysis, a QC sample of diluted composite injectate solution was measured every ten samples.

Dissolved Metals Analyses

Dissolved Al, B, Ca, Cr, Cu, Fe, K, Mg, Mn, Na, Ni, P, Pb, Si, and Zn were analyzed by inductively-coupled plasma atomic emission spectroscopy (ICP-AES) (Coston et al., 1998). Method detection limits, determined by making repeated measurements of solutions spiked at 5 and 10 times the instrument detection limit, for the tracers are listed in Table 4. Samples with concentrations greater than 150 mM were diluted and reanalyzed. A QC sample was run every 10-15 samples and five samples of diluted composite injectate solution were measured for each analytical run. Metals analyses were completed within one to three months of each sampling round. Thc concentration of P measured by ICP-AES was equivalent to orthophosphate measured colorometrically in groundwater from the field site by the ascorbic acid-molybdenum blue method (Rea et al., 1996).

Methods for Calculation of Moments

Spatial Moments

A spatial-moments approach was used to quantify the transport of the injected solutes through the aquifer, providing estimates of tracer mass, location, velocity, and other transport parameters, not discussed here, such as dispersivity. The three-dimensional spatial moments of the following forms were used to calculate the total mass and center of mass:

Total Mass (zeroth moment):

$$M = \iiint_{\Omega} nC_i \, dxdydz \tag{1}$$

1st Moment:

$$M_{ijk} = \iiint_{\Omega} x^i y^j z^k nC_i \, dxdydz \tag{2}$$

Center of Mass:

$$\bar{x} = \frac{M_{100}}{M}; \bar{y} = \frac{M_{010}}{M}; \bar{z} = \frac{M_{001}}{M} \tag{3}$$

where Ω is the test domain; i, j, and k are 0 or 1; n is the porosity, C_i is the concentration of solute i, and x, y, and z are spatial coordinates.

The data set for each synoptic sampling contains location (x, y, and z) and concentration data. Because the data are spatially discontinuous, numerical approximations to Equations 1 and 2 were required. The initial step in the moments analysis was an integration in the vertical direction (z) at each MLS. As many as 15 samples were taken at different altitudes in the aquifer at the same x, y location, providing good definition of the vertical distribution of tracers. Linear changes in concentration were assumed between sampling points along each vertical profile.

Following the vertical integration, a horizontal integration was performed. The horizontal spacing between MLS was much greater than the vertical spacing between sampling points along an MLS. To conduct the numerical integration the horizontal plane was divided into contiguous triangular regions with the apex of each triangle defined by a sampled MLS. Linear interpolation over these triangular regions then completed the calculations. Details of this integration approach are given in Garabedian et al. (1991).

Temporal Moments

Areas under the breakthrough curves (the zeroth moments) were calculated using the trapezoidal rule (no smoothing function), following the approach and equations given in Kent et al. (1994, 1995). Average travel time (the first moment) for each tracer, $\langle t_i \rangle$, was calculated according to the equation given by Roberts et al. (1986):

$$\langle t_i \rangle = \frac{\sum_{j=1}^{m} \left(C_{i,j} / C_{i,0} \right) t_j}{\sum_{j=1}^{m} \left(C_{i,j} / C_{i,0} \right)} \tag{4}$$

where m is the number of data points, $C_{i,j}$ is the concentration of solute i of data point j, $C_{i,0}$ is the injected concentration of solute i, and t_j is the number of days since injection. The mean retardation factors for individual tracers, $R_{f,i}$, are estimated by dividing the average travel time for each tracer, $\langle t_i \rangle$, by the average time for the conservative tracer, $\langle t_{Br} \rangle$. Longitudinal dispersivity (the second moment) for the conservative tracer, Br, was calculated using the definition of Harvey and Garabedian (1991):

$$\alpha_L = x_l \frac{\left(\Delta t / t_{pk} \right)^2}{16 \ln 2} \tag{5}$$

where x_l is the distance to the breakthrough MLS in meters, Δt is the peak width at half peak height, and t_{pk} is the time to the peak of the breakthrough curve. The relationship is only valid if Br does not adsorb and the ratio a_L/x_l is small (<0.01).

Results and Discussion

Bromide Transport

Conservative, non-reactive transport of Br has been observed at this site in many small-scale tests and in one other large-scale test conducted in 1985-88 (LeBlanc et al., 1991; Garabedian et al., 1991). Thus, Br was expected to travel through the aquifer without interacting with the sediments. In this section we describe the observed Br transport, present results of the moments analysis of the Br distribution, and compare these results with those from the 1985-88 test.

The Br tracer cloud was followed for 210 days after injection; later in the test, parts of the Br tracer cloud moved beyond the instrumented region of the aquifer. The left-hand portion of Figure 5 shows the mapped distribution of maximum Br observed after 13 and 83 days of transport. With time, the tracer cloud lengthened in the direction of transport. The longitudinal length of the tracer cloud, as defined by the 0.002 relative concentration (C/C_o) contour, was 15 and 50 m at 13 and 83 days, respectively. The spread of tracer in the directions perpendicular to flow was much less. The horizontal width of the Br cloud was approximately 8 m at both 13 and 83 days, whereas the initial width of the cloud was estimated to be about 4 m.

The Br tracer cloud was well defined in the vertical direction, because of the close vertical spacing of sampling ports on the MLS. As shown in longitudinal cross sections (Figure 6) the height of the tracer cloud was approximately 4 and 6.5 m at 13 and 83 days, respectively. The initial vertical extent of the tracer cloud was estimated to be about 3.5 m (Table 2). By 83 days the Br tracer cloud had developed an asymmetrical vertical distribution with the leading edge traveling relatively high and the trailing edge lower in the aquifer. This asymmetry was probably caused by local variability in hydraulic conductivity. The variability in hydraulic conductivity also may account for part of the large vertical spreading of the cloud observed between 13 and 83 days (Figure 6). The vertical sinking of the tracer cloud early in the test, discussed below, may also contribute to the early vertical spreading of the Br tracer cloud.

Spatial-Moments Analysis for Bromide

The zeroth moment quantifies the total mass within the tracer cloud. The porosity assumed in the analysis (Equation 1) affects the estimated mass. A constant porosity of 0.39, used by Garabedian et al. (1991) in the analysis of the previous large-scale test, was used here also. Figure 7 shows the estimated mass of Br for each synoptic sampling; the estimated mass ranged from 0.89 to 1.19 times the injected Br mass, with an average of 1.03 for the eight synoptic samplings. No temporal trend was observed, indicating that the Br tracer traveled conservatively and did not interact with the aquifer sediments. The deviations of estimated mass from the injected mass were probably derived from the spatially discontinuous nature of the sampling and the numerical approximations made in the moments analysis.

All water pumped to clear the MLS tubing before sampling and for rinsing sample bottles was captured in large waste containers during each spatial sampling. The volume of the water and its tracer concentrations were measured to account for tracer mass removed by the pumping and sampling activities. Summed over the entire tracer test, approximately 0.8% of the Br and Ni tracer masses were removed by the sampling activities, which is well within the observed variation in calculated masses caused by other problems, such as insufficient sampling on the sides of the tracer cloud or mass estimation errors caused by the linearization of concentration gradients in the spatial analyses.

The first moment quantifies the location of the center of the tracer cloud. The porosity assumed in the calculations does not affect the first moment results because the porosity appears in both the numerator and denominator of Equation 3. This is the case for all first and higher moments. Figure 8 shows the relation of the distance traveled (location of the center of mass relative to the injection center) to the time traveled in the aquifer for the Br cloud. A linear regression applied to this relation yields a velocity estimate of 0.47 m/d. The scatter around the regression line is small (Figure 8a) and the correlation coefficient of the relation is very high ($r = 0.999$), implying that the average velocity was constant throughout the test.

The water-table altitude fluctuated about 0.8 m during the 12 months of the tracer test (April 1993 to March 1994) with the highest and lowest altitudes occurring in May 1993 and December 1993, respectively (Figure 9). This observed pattern is typical of the seasonal fluctuations in the water table observed over ten years at this site. The direction of the water-table gradient also varied seasonally about 16 degrees, with more southerly and easterly directions corresponding to periods of low and high water levels, respectively (Figure 9a). The water-table gradient magnitude varied between 1.5 and 1.9 m per 1000 m and lagged slightly behind altitude in its seasonal pattern (Figure 9b).

Mapping the centers of mass (Figure 10) shows a slightly curved trajectory over which the tracer cloud traveled. This curved trajectory is also reflected in the general path of transport shown in Figure 3. Early in the test the flow path was more easterly. Contour maps of the water-table surface also are shown in Figure 10 for 48 and 239 days after injection; the directions of ground-water flow, estimated from the water-table contours, differ by 14.5 degrees between the two observations. The change in the direction of transport of the Br tracer cloud center of mass agrees with observed change in the water-table gradient direction.

The vertical location of the Br cloud over time is shown along a cross section in Figure 11. Downward movement of the tracer cloud was observed over the first 111 days. The vertical altitude of the center of mass dropped 1.9 m from 12.2 m at the center of the injection interval at 0 days, to 10.3 m at 111 days. A primary cause of this drop in altitude was the greater density of the tracer cloud relative to the native groundwater. As the cloud was diluted over time through dispersion, this density contrast diminished and the amount of sinking decreased.

Seasonal changes in hydrologic conditions may have influenced the vertical trajectory of the tracer cloud. Although the vertical hydraulic gradients were too small to be detected in this section of the aquifer, a seasonal pattern in vertical hydraulic gradient is consistent with other observed seasonal changes in hydrologic conditions. The injection was made during the spring (April) when recharge to the aquifer from precipitation is estimated to be occurring (Barlow and Hess, 1993). This recharge would create a downward vertical hydraulic gradient, which may be smaller than can be easily detected. In the summer, potential evapotranspiration generally exceeds precipitation. Thus, by 100 days after the injection (July), recharge to the aquifer should have been limited, and the vertical hydraulic gradient minimized. Hence, the seasonal changes in recharge may have caused changes in the vertical hydraulic gradient and in the vertical trajectory. Any effect of recharge-induced sinking on the tracer cloud would be in addition to the effects of density.

Temporal-Moments Analysis for Bromide

The results of the breakthrough well sampling for Br are presented in Table 5 for both MLS sampled. Bromide was detectable over 5.34 m of vertical altitude in BT1 and 5.58 m in BT2, which was 15 meters farther downgradient. Representative breakthrough curves for Br, EDTA, and Ni in the different geochemical zones in the aquifer are shown in Figure 12. The Br peaks are symmetric and have a similar shape at all depths; this is consistent with the expected behavior of a conservative tracer. Bromide breakthrough did not occur simultaneously at all depths; the pattern of Br breakthrough is consistent with the longitudinal cross section through the cloud shown in Figure 6. Differences in peak appearance times are attributed to local variations in the horizontal hydraulic conductivity of the aquifer. Variations in the

horizontal hydraulic conductivity are expected on the order of the spacing of the MLS sampling ports because the sediments were deposited in layers that are on the order of 30 centimeters thick (Hess et al., 1992).

Longitudinal dispersivities calculated from the breakthrough well data are considerably smaller than the value calculated from the synoptic data sets. Longitudinal dispersivities in the breakthrough MLS vary from 0.01 to 0.51 meters, compared to the 2.2 meters calculated from the synoptic data (Hess et al., 1999). Calculated dispersivities for Br from Equation 5 agree with values reported from small-scale tracer tests at the Cape Cod site (Harvey and Garabedian et al., 1991; Kent et al., 1994, 1995), but they are significantly less than the 0.96 m calculated for the other large-scale test conducted at this site (Garabedian et al., 1991). The volume of aquifer sampled by each port of the breakthrough MLS is small and thus the dispersivities calculated from the breakthrough MLS are representative of small-scale heterogeneities in hydraulic conductivity. BT1 has more variability from depth to depth than BT2. The largest dispersivity values occurred above 9.85 meters altitude and are consistent with the cloud elongation shown in the vertical cross sections through the Br tracer cloud (Figure 6).

Comparison of Bromide Results to an Earlier Tracer Test (1985-1988)

A tracer test of similar magnitude was conducted at this site in 1985-1988 (LeBlanc et al., 1991; Garabedian et al., 1991). The primary purpose of that test was to investigate the dispersion of a nonreactive solute as it traveled through a heterogeneous aquifer. The injection location for the earlier test was 43 m upgradient from that of the current test. Consequently, the sections of aquifer traversed in the two tests are different but they overlap. A comparison between the results of the 1985-1988 and the current test provides insight into the stationarity of transport properties in this aquifer.

The synoptic sampling and spatial-moments analysis approach provided good characterizations of the distribution of Br tracer in both tests. The average normalized mass for the 1985-88 test was 0.97, as compared to 1.00 for the current test. Although the plots of distance traveled against time are very similar for the two tests (Figure 8b), the mean velocities determined from the location of the center of mass with time are slightly different. Garabedian et al. (1991) reports a velocity of 0.42 m/d with a correlation coefficient of 0.997 for the earlier test. The velocity reported above for the current test is 0.47 m/d with a correlation coefficient of 0.999. Assuming that the hydraulic conductivity was the same for the two tests, the 12% increase in velocity can be explained by the slight difference in hydraulic gradient during the two tests (Figure 13). On average, the gradient magnitude was about 0.18 m per thousand meters higher during the current test than in the 1985-1988 test, which is a 12% increase in magnitude.

The two experiments, although conducted in different sections of the aquifer, provide similar estimates of the mean properties of the aquifer. The use of a constant porosity (0.39) in the spatial-moments analysis estimated near 100% mass recovery, which supports conservative, non-reactive transport of Br in both experiments. This estimate of porosity is within the range expected for this type of coarse sand and gravel deposit. The velocities estimated from the two tests are also similar, suggesting that the mean horizontal hydraulic conductivity is the same throughout the aquifer. In subsequent reports, comparisons of the results of the second-moments analysis will provide information on the spatial stationarity of solute dispersion in this aquifer.

Similar density-dependent transport behavior was observed in the two tests (Figure 14). Both tracer clouds sank extensively during the first 100 days of transport. The tracer cloud in the earlier experiment continued to sink until about 237 days after injection. Seasonal differences in recharge may account for this difference in vertical sinking; the 1985-1988 test began in July and the 1993-1994 test began in April.

Tracer-induced Perturbations in Groundwater pH Values

Chemical reactivity is a function of pH, therefore it is important to understand how the existing pH conditions may have been altered during the tracer test. The injection of the tracer solution temporarily changed the pre-existing pH gradient because the injectate solution had a uniform pH of 5.6 (Table 2, Figure 2). In addition, several different chemical reactions between solutes in the tracer cloud and the aquifer sediments could also cause local changes in pH values.

Exchange reactions, chromate reduction and metal ion adsorption would all result in a net consumption of hydrogen ions (H^+), and therefore an increased pH. Exchange of the metal ion in the injected metal-EDTA complexes with Fe(III) dissolved from oxyhydroxide phases would be accompanied by adsorption of the metal ion and consumption of H^+ ions:

$$MeEDTA^{2-} + Fe(OH)_{3,s} + >SOH + 2H^+ = FeEDTA^- + >SOMe^+ + 3H_2O \quad (6)$$

where Me represents a divalent metal initially complexed with EDTA in the tracer solution and >SOH represents an adsorption site on the aquifer sediments. Metal exchange reactions of the EDTA complexes with Al would have the same stoichiometry. Reduction of Cr(VI) by Fe(II) could be accompanied by consumption or production of H^+, depending on the chemical speciation of Fe(II). For example, reduction of Cr(VI) by magnetite results in the consumption of H^+:

$$3Fe_3O_{4,s} + CrO_4^{2-} + 14H_2O + 2H^+ = 9Fe(OH)_{3,s} + Cr(OH)_{3,s} \quad (7)$$

Reduction of Cr(VI) by other Fe(II) minerals, such as glauconite, would also consume H^+. The results of Anderson et al. (1994) suggest that the reaction in Equation 7 was more likely to be the dominant pathway for Cr(VI) reduction in the aquifer.

Observations suggest that the net result of chemical reactions between reactive tracers and aquifer sediments led to a net decrease or negligible change in pH values. It is likely that the decrease in pH resulted from ion exchange reactions of major ions in the tracer cloud with the aquifer sediments, which caused a net release of H^+. The sodium ion (Na^+) concentration of the injectate solution was greater than 4.4 mM (Table 1). The Na^+ concentration of the ambient groundwater ranged from less than 200 mM in the pristine zone to about 2 mM in the suboxic zone. The potassium ion (K^+) concentration in the injectate solution was also about 4.4 mM (Table 1). In contrast, the K^+ concentration in ambient groundwater ranged from about 11 μM in the pristine zone to about 300 μM in the suboxic zone (Kent et al., 1994). These monovalent cations undergo weak interactions with surface sites on oxide minerals (Davis and Kent, 1990) accompanied by the release of H^+:

$$>SOH + K^+ = >SO^-K^+ + H^+ \quad (8)$$

In addition to H^+, weakly adsorbed divalent cations, such as Ca^{2+} and Mg^{2+}, on oxide or aluminosilicate surfaces could exchange with dissolved Na^+ and K^+ in the tracer cloud. Such reactions have already been shown to cause the retardation of lithium ions in the aquifer (Wood et al., 1990).

The magnitude of the ion exchange reactions should decrease from the pristine zone to the suboxic zone as a result of the increase in cation concentrations with depth. In the pristine zone close to the injection, the experimental data show that reactions between the tracer cloud and the sediments caused a decrease in pH (Figure 15; Table 2). Breakthrough of the tracers at concentrations close to their values in the injectate solution was accompanied by a decrease in pH from approximately 5.8 to 5.2. Coincident with the decrease in pH, there was an increase in the concentrations of Na^+, K^+, Ca^{2+}, and Mg^{2+} (Figure 15). Concentrations of Na^+ increased to values close to those in the injectate, but K^+ concentrations were much less than those in the injectate (Figure 15). Thus, it is likely that reactions similar to those represented by Equation 8 caused the observed decrease in pH and that K^+ was a more important reactant than Na^+.

Perturbations in pH values in the pristine zone were still measurable 37 m downgradient at BT1 (Figure 16). The decrease in pH was observed along the rising limb of the breakthrough curve, indicating that it was a feature associated with the leading edge of the tracer cloud. Other small fluctuations in pH were observed after the rising limb of the Br breakthrough curve; but most of these were within the error of the measurement (±0.15 pH units). During breakthrough of the reactive tracers in the pristine zone (at about 90 days, c.f. Figure 12A), the pH values were close to those in the ambient groundwater.

No significant change in pH was observed at lower altitudes in the aquifer (Figure 17). In addition to the greater importance of K^+ exchange with Ca^{2+} and Mg^{2+} in the suboxic zone, alkalinities in the suboxic zone of the sewage plume are up to 20 times larger than those in the pristine zone (LeBlanc et al., 1991). Thus, as a result of both the greater buffer capacity of the groundwater and the higher concentrations of exchangeable divalent cations, the tracer cloud did not cause significant pH perturbations in the suboxic zone.

EDTA Speciation

Only the six metals, Cu, Ni, Pb, Zn, Fe, and Al, were complexed with EDTA. Neither Mn-EDTA nor any other metal-EDTA complexes formed to an appreciable extent after the injection, as indicated by analysis of the speciation samples. Thus, there was an excellent correlation between the measured EDTA concentration (from samples collected at the breakthrough MLS and for the selected synoptic transect samples for which speciation was determined) and the sum of the total concentrations of dissolved Cu, Ni, Pb, Zn, Fe, and Al as measured by ICPAES (Figure 18). The summation method should slightly overestimate the EDTA mass because a portion of the dissolved Zn is not complexed (Davis et al., 2000), however, the sum of the six dissolved metals was generally about 3% less than the measured EDTA concentration (Figure 18). Therefore, in the absence of measured EDTA concentrations for each point in the synoptic samplings, the sum of the six metals is a reasonable method for estimating dissolved EDTA mass during the experiment.

EDTA was transported not as uncomplexed $EDTA^{4-}$, but as a collection of anionic metal-EDTA complexes. Although subsequent discussion refers to the “Ni cloud”, Ni is actually present as dissolved Ni-EDTA (Table 2). The overall result of the metal exchange reactions that occurred as the tracer cloud moved downgradient was a shift in the EDTA speciation among the four injected metals (Ni, Pb, Cu, Zn) and the two metals derived from oxide dissolution, Al and Fe(III) as described by Equation 6, above. By the end of the experiment, EDTA speciation was dominated by the Fe- and Ni-EDTA complexes (Figure 19).

The synoptic sampling at 175 days showed a much higher estimate of EDTA mass than any of the other samplings. The sampling at 175 days was the only one conducted during a heavy rainstorm, and the wet conditions appeared to cause problems with contamination of sample containers and filtered samples with sand grains and other inorganic detritus that adhered to plastic gloves and the sampling equipment. After acidification of the samples, metals associated with this

particulate matter could be dissolved under the acidic conditions in the samples. This appeared to cause a particular problem with the concentrations of dissolved Fe observed during this sampling, and can be seen in the large dissolved Fe mass found at 175 days (Figure 19). The masses of other tracers at the 175 day sampling fell closer to the general trends observed as a function of time. This is consistent with the results of a comparison of metal ion concentrations in filtered and unfiltered samples conducted elsewhere in the aquifer, which showed that the only metal ion for which significantly higher concentrations were observed in unfiltered samples was Fe (Kent, 1998).

Unlike the mass of dissolved Al, which decreased rapidly with time during the test, the mass of dissolved Fe in the EDTA tracer cloud increased steadily (Figure 19), consistent with the known thermodynamic stability of the Fe(III)-EDTA complexes. At chemical equilibrium, the degree of exchange of the four injected metals with Fe(III) is different for each metal and is dependent primarily on pH and the concentration of the metal-EDTA complexes. Nickel was expected to be the least reactive of the four injected metal-EDTA complexes because it had the largest stability constant (Martell and Smith, 1989). The exchange reaction is more favorable as the concentration of metal-EDTA complexes decreases. Thus, dilution of the tracer cloud by dispersion enhances the exchange reaction with Fe(III) and would cause a general increase in dissolved Fe mass as the tracer test progressed (Figure 19).

Comparison Between Ni, EDTA, and Br Transport

As was the case for Br, the Ni tracer cloud lengthened in the direction of transport as these solutes were transported through the aquifer, although it lengthened less than the Br cloud (longitudinal lengths of the Ni cloud were 14 and 45 m at 13 and 83 days, respectively) (Figure 5). The horizontal width of both tracer clouds, based on the 0.002 relative concentration contour at 13 and 83 days, was about 8 m, as compared to the initial width of 4 m. Because of the method used for estimating EDTA in the spatial samplings (discussed above), contour plots were not made for this constituent.

The Ni cloud also moved downward over the first 111 days of the test. Initially the injection straddled the Zn-contaminated region, and as the test progressed, the tracers sank such that the center of mass traveled toward the lower boundary of the Zn-contaminated region (Figure 20). The Zn-contaminated region thins about 75 m downgradient of the injection site (Figure 2). By the last spatial sampling (314 days) the center of Ni mass had sunk out of the Zn-contaminated region. As described previously, this downward movement was likely caused by a density contrast between the tracer solution and ambient groundwater and immeasurable, downward gradients resulting from recharge derived from precipitation.

Spatial-moment and temporal-moment analyses were performed on the concentration data to quantify the transport of the EDTA and Ni tracer through the aquifer. Figure 21a displays the EDTA, Ni and Br masses through time, as calculated by the zeroth moment analysis of the sampled distributions and each normalized by dividing by their respective injection mass. The normalized Br masses cluster around the line that defines conservative transport (1.0). The normalized Ni masses all fall below 1.0, implying that some Ni was removed from the groundwater by adsorption to the aquifer sediments. The estimated normalized mass of Ni ranges from 0.76 to 0.97, with an average mass of 0.88 (for nine synoptic samplings). EDTA estimated mass was generally less than 1.0 early in the tracer test due to adsorption of metal-EDTA complexes. The calculation from summation of the metal masses likely overestimated EDTA mass as the tracer cloud area increased, because total Zn mass includes both Zn-EDTA and uncomplexed Zn masses (discussed above and in Davis et al., 2000). Moments calculated from breakthrough curves for EDTA and Ni indicated reversible adsorption: both tracers were retarded but areas under their breakthrough curves were similar to those for Br (Figures 12 and 24).

In a second normalization step, each normalized Ni or EDTA mass was divided by the corresponding normalized Br mass to obtain a relative mass (Figure 21b). This second normalization was done to remove error in the calculated masses that might result from the spatial sampling scheme. The relative masses for Ni clustered around an average of 0.87 and for EDTA averaged 0.99 (for eight synoptic samplings).

When the observed concentration data are displayed along a longitudinal cross section (Figure 6), significant differences between the Ni and Br distributions are apparent. The two clouds were both about 4 and 6.5 m in vertical thickness at 13 and 83 days, respectively, compared to the initial thickness of about 3 m; but the shapes of the clouds differed substantially. The leading edge of the Ni cloud at 83 days trails behind the leading edge of the Br cloud and is located lower in the aquifer in the transition zone (Figure 6). In the upper portion of the aquifer, the trailing edge of the Ni tracer cloud is far behind the trailing edge for Br. Regression analysis of the center-of-mass locations of the tracers with time (Figure 22) estimated the velocity of the Ni tracer at 0.39 m/d (n=10, r=0.998). Thus the average retardation factor (R_f) was 1.2 for Ni transport relative to Br.

An areal map of the centers of mass of the Ni and Br clouds with time (Figure 23) shows how Ni lagged behind Br. This lag and the changes in the direction of the hydraulic gradient over the period monitored (Figure 9a) resulted in the two tracer clouds, Ni and Br, diverging onto slightly different trajectories. The centers of mass for the Br and Ni clouds at 175 and 210 days, respectively, are located near each other (Figure 23); however, the Ni center of mass for 210 days is located slightly to the west of the Br center for 175 days. The direction of ground-water flow, based on the estimated

hydraulic gradient, changed 4.8 degrees over the 35 days between the two samplings, and resulted in the observed difference in trajectories.

Adsorptive losses of Ni and EDTA masses were evident early in the test. Between the time of the injection and the first spatial sampling 13 days later, about 15% of both the EDTA mass (expressed as the sum of the six metals) and Ni mass were adsorbed onto the aquifer sediments (Figure 21b). Based on the speciation sampling completed throughout the test, dissolved Ni mass was transported as the anionic complex $NiEDTA^{2-}$. After this initial loss, both the EDTA and Ni masses were fairly constant (Figures 19, 21b, and 24a). By the time the tracer cloud reached the breakthrough wells (45 days after injection) the normalized areas under the breakthrough curves for Br, EDTA, and Ni were approximately equal (Figure 24a) indicating that adsorption of the EDTA and Ni-EDTA complexes was reversible. Thus, EDTA and Ni-EDTA transport through the aquifer were retarded by adsorption, but the masses being transported were nearly constant after the initial equilibration of the tracers with the aquifer solids.

Complicating an analysis of the effects of small-scale heterogeneity was the large-scale variable adsorption of Ni onto the aquifer sediments in the different geochemical zones of the aquifer (Figures 6, 12, and 24b). The difference in cloud shape between Ni and Br (Figure 6) was consistent with the delayed peak appearance and long trailing edges of the breakthrough curves for EDTA and Ni-EDTA in Figure 12a. Both EDTA and the divalent Ni-EDTA complexes were more retarded in the pristine zone (Figure 24b). Adsorption of the metal-EDTA complexes was greater in the pristine zone near the water table, because the pH is lower (around 5.5) than in the suboxic zone of the aquifer. In addition, the concentrations of other anions, such as sulfate and phosphate, which compete with the divalent metal-EDTA complexes (i.e., Ni-EDTA) for available adsorption sites, are low in the pristine zone. However, Ni-EDTA was consistently more retarded than EDTA. Retardation factors up to 2.07 were measured for Ni-EDTA in the pristine zone as compared to 1.34 for the total EDTA peak. Monovalent Fe(III)-EDTA complexes were retarded less than the divalent Ni-EDTA complexes (Davis et al., 2000), decreasing the retardation represented by the total EDTA peak in the pristine zone. Under the geochemical conditions of the sewage-contaminated zone, total EDTA and divalent Ni-EDTA were retarded similarly, indicating similar extents of adsorption for the divalent Cu-, Ni-, and Zn-EDTA complexes (Pb did not breakthrough) and monovalent (Fe-, Al-EDTA) complexes present (Figure 24b).

Summary

Comparisons between the distributions of conservative and weakly reactive tracers showed how small- and large-scale geochemical and hydrogeological heterogeneity may affect solute transport. The following general conclusions were reached.

1. Bromide ion was transported conservatively during the experiment. The results for the current test compare favorably with the Br transport parameters calculated from a previous large-scale tracer test at the site. Based on spatial moments analysis of eight synoptic data sets the average normalized mass for Br was 1.03 and the mean velocity was 0.47 m/d.
2. Injection of the tracer cloud induced only minor changes in the chemical conditions in the aquifer. The most significant change was a small decrease in pH in the pristine zone, most likely resulting from ion exchange reactions. The impact of this change on transport of reactive tracers was only significant early in the tracer test.
3. EDTA can be represented as the sum of 6 dissolved metals: Al, Fe, Cu, Ni, Pb, and Zn. Complexes with these metal ions comprised 100% of the EDTA throughout the tracer test.
4. The metal-EDTA complexes, including Ni-EDTA, were reversibly adsorbed onto the aquifer solids during transport.
5. Transport of the metal-EDTA complexes was highly retarded in the pristine zone and only slightly retarded in the transition and suboxic zones.
6. Due to the sinking of the tracer cloud, the percentage of each tracer that traveled in each geochemical zone varied over time. Early in the test more of the tracer was located high in the aquifer in the pristine zone, but with time, the sinking caused less tracer to be in the pristine zone and more to be in the suboxic zone.
7. Attempts to quantify the effects of small-scale heterogeneity on transport are complicated because the Br and Ni-EDTA tracer clouds encountered different sections of the aquifer as they traveled downgradient along slightly different trajectories.

References

Anderson, L.D., Kent, D.B., and Davis, J.A. (1994) Batch experiments characterizing the reduction of Cr(VI) using suboxic material from a mildly reducing sand and gravel aquifer, Environ. Sci. Technol., 28(1), 178-185.

Barber, L.B., II, Thurman, E.M., Schroeder, M.P., and LeBlanc, D.R. (1988) Long-term fate of organic micropollutants in sewage-contaminated groundwater, Environ. Sci. Technol., 22(2), 205-211.

Barber, L.B., II, Thurman, E.M., and Runnells, D.D. (1992) Geochemical heterogeneity in a sand and gravel aquifer: Effect of sediment mineralogy and particle size on the sorption of chlorobenzenes, J. Contam. Hydrol., 9(1), 35-54.

Barlow, P.M. (1987) The use of temperature as a ground-water tracer in glacial outwash: Tucson, Ariz., University of Arizona, Dept. of Hydrology and Water Resources, unpublished M.S. thesis, 141 pp.

Barlow, P.M., and Hess, K.M. (1993) Simulated hydrologic responses of the Quashnet River stream-aquifer system to proposed ground-water withdrawals, Cape Cod, Massachusetts, U.S. Geological Survey Water-Resources Investigations Report 93-4064, 52 pp.

Bhattacharyya, S.N. and Kunda, K.P. (1971) Spectrophotometric determination of EDTA, Taranta, 18, 446-449.

Borggaard, O.K. (1991) Effects of phosphate on iron oxide dissolution in EDTA and oxalate, Clays and Clay Min., 39(3), 321-325.

Bowers, A.R. and Huang, C.P. (1986) Adsorption characteristics of metal-EDTA complexes onto hydrous oxides, J. Colloid Interface Sci., 110(2), 575-590.

Cederberg, G.A., Street, R.L., Leckie, J.O. (1985) A groundwater mass transport and equilibrium chemistry model for multicomponent systems, Water Resour. Res., 21(8), 1095-1104.

Coston, J.A., Fuller, C.C., and Davis, J.A. (1995) Pb^{2+} and Zn^{2+} adsorption by a natural aluminum- and iron-bearing surface coating on an aquifer sand, Geochim. Cosmochim. Acta, 59(17), 3535-3547.

Coston, J.A., Abrams, R. H., and Kent, D. B. (1998) Selected inorganic solutes, *in* Savioe, J. and LeBlanc, D. R., Eds., Water-quality data and methods of analysis for samples collected near a plume of sewage-contaminated ground water, Ashumet Valley, Cape Cod, Massachusetts, 1993-94, U.S. Geological Survey Water-Resources Investigations Report 97-4269, 19-21.

Curtis, G.P. and Rubin, J., submitted, Solute transport influenced by multiple, equilibrium controlled reactions: Extensions and numerical implementation of the feed forward method to complex reaction networks, submitted to Water Resour. Res.

Davis, J. A., Coston, J. A., Kent, D. B., and Fuller, C. C. (1998) Application of the surface complexation concept to complex mineral assemblages, Environ. Sci. Technol., 32, 2820-2828.

Davis, J.A., Coston, J.A., Kent, D.B., Hess, K.M., Joye, J.L., Brienen, P., and Bussey, K.W. (2000) Multispecies reactive tracer test in a sand and gravel aquifer, Cape Cod, Massachusetts. Part II. Transport of chromium(VI) and lead-, copper-, and zinc-EDTA tracers, EPA/600/R-01/007b, 47 pp., U. S. Environmental Protection Agency.

Davis, J.A., Kent, D.B., Rea, B.A., Maest, A.S., and Garabedian, S.P. (1993) Influence of redox environment and aqueous speciation on metal transport in groundwater: Preliminary results of tracer injection studies, *in* Allen, H.E., Perdue, E.M, and Brown, D.S., Eds., Metals in Groundwater, Chelsea, MI, Lewis Publishers, 223-273.

Davis, J.A. and Kent, D.B. (1990) Surface complexation modeling in aqueous geochemistry, Rev. Mineral., 23, 177-260.

Foerstner, U., and van Lierde, J.H. (1983) Trace metals in water purification processes, *in* Foerstner, U. and Wittman, T.W., Eds., Metal Pollution in the Aquatic Environment, New York, Springer-Verlag, 324-359.

Franson, M.A.H (1985) Standard methods for the examination of water and wastewater, 16th ed. American Public Health Association, Washington, D.C., 201-204.

Garabedian, S.P. (1987) Large-scale dispersive transport in aquifers: Field experiments and reactive transport theory: Cambridge, Mass., Massachusetts Institute of Technology, Dept. of Civil Engineering, PhD thesis, 290 pp.

Garabedian, S. P., LeBlanc, D. R., Gelhar, L. W., and Celia, M. A. (1991) Large-scale natural gradient tracer test in sand and gravel, Cape Cod, Massachusetts, 2. Analysis of spatial moments for a nonreactive tracer, Water Resour. Res., 27(5), 911-924.

Harvey, R.W. and Garabedian, S.P. (1991) Use of colloid filtration theory in modeling movement of bacteria through a contaminated sandy aquifer, Environ. Sci. Technol., 25(1), 178-185.

Hess, K. M., Davis, J. A., Coston, J. A., and Kent, D. B., 1999, Multspecies reactive transport in an aquifer with spatially variable chemical conditions: Dispersion of bromide and nickel tracers, *in* Morganwalp, D.W., and Buxton, H.T., Eds., U.S. Geological Survey Toxic Substances Hydrology Program—Proceedings of the Technical Meeting,

Charleston, South Carolina, March 8-12, 1999 — Volume 3 — Subsurface Contamination from Point Sources: U.S. Geological Survey Water-Resources Investigations Report 99-4018C, pp. 393-404.

Hess, K.M., Wolf, S.H., and Celia, M.A. (1992) Large-scale natural gradient tracer test in sand and gravel, Cape Cod, Massachusetts: 3. Hydraulic-conductivity variability and calculated macrodispersivities, Water Resour. Res., 28(8), 2011-2027.

Hostetler, C. J., Erikson, R.L., Fruchter, J.S., and Kincaid, C.T. (1989) FASTCHEM package, Overview and application to a chemical transport problem, Final Report for EPRI EA-5870, Project 2485-2, Pacific Northwest Lab, Richland, WA.

Huang, C.P., Rhoads, E.A., Hao, O.J. (1988) Adsorption of Zn(II) onto hydrous aluminosilicates in the presence of EDTA, Water Res., 22(8), 1001-1009.

Kent, D. B., 1998, Effects of pumping rate and filtration on measured concentrations of inorganic solutes, *in* J. Savioe and D. R. LeBlanc, Eds., Water-quality data and methods of analysis for samples collected near a plume of sewage-contaminated ground water, Ashumet Valley, Cape Cod, Massachusetts, 1993-94, U.S. Geological Survey Water-Resources Investigations Report 97-4269, 11-15.

Kent, D. B., Abrams, R. H., Davis, J. A., Coston, J. A., and LeBlanc, D. R. (2000a) Modeling the influence of variable pH on the transport of zinc in a contaminated aquifer using semi-empirical surface complexation models, Water Resour. Res., 36, 3411-3425.

Kent, D.B., Davis, J.A., Anderson, L.C.D., and Rea, B.A. (1995) Transport of chromium and selenium in a pristine sand and gravel aquifer: Role of adsorption processes, Water Resour. Res., 31(4), 1041-1050.

Kent, D.B., Davis, J.A., Anderson, L.C.D., Rea, B.A., and Waite, T.D. (1994) Transport of chromium and selenium in the suboxic zone of a shallow aquifer: Influence of redox and adsorption reactions, Water Resour. Res., 30(4), 1099-1114.

Kent, D.B., Davis, J.A., Rea, B.A., and Anderson, L.C.D. (1992) Ligand-enhanced transport of strongly adsorbing metal ions in the ground-water environment, *in* Kharaka, Y. and Maest, A.S., Eds., Water-Rock Interactions WRI-7, Rotterdam, A.A. Balkema, 1, 805-808.

Kent, D.B., Davis, J.A., Anderson, L.C.D., Rea, B.A., and Coston, J.A., (2000b) Effect of adsorbed metal contaminants on the transport of Zn- and Ni-EDTA complexes in a sand and gravel aquifer, Environ. Sci. Technol., submitted.

Kent D. B. and Maeder, V., 1999, Evolution of a ground-water sewage plume after removal of the 60-year-long source, Cape Cod, Massachusetts: pH and fate of phosphate and metals, *in* Morganwalp, D.W., and Buxton, H.T., Eds., U.S. Geological Survey Toxic Substances Hydrology Program—Proceedings of the Technical Meeting, Charleston, South Carolina, March 8-12, 1999 — Volume 3 — Subsurface Contamination from Point Sources: U.S. Geological Survey Water-Resources Investigations Report 99-4018C, pp. 245-259.

Kohler, M., Curtis, G.P., Kent, D.B., and Davis, J.A. (1996) Experimental investigation and modeling of uranium(VI) transport under variable chemical conditions, Water Resour. Res., 32(12), 3539-3551.

LeBlanc, D.R., Garabedian, S.P., Hess, K.M., Gelhar, L.W., Quadri, R.D., Stollenwerk, K.G., and Wood, W.W. (1991) Large-scale natural gradient tracer test in sand and gravel, Cape Cod, Massachusetts: 1. Experimental design and observed tracer movement, Water Resour. Res., 27(5), 895-910.

LeBlanc, D.R., Guswa, J.H., Frimpter, M.H., and Londquist, C.J. (1986) Ground-water resources of Cape Cod, Massachuetts, U.S. Geological Survey Hydrologic Investigations Atlas, HA-692, 4 sheets.

LeBlanc, D.R. (1984) Sewage plume in a sand and gravel aquifer, Cape Cod, Massachusetts, U.S. Geological Survey Water-Supply Paper, 2218, 28 pp.

Liu, C.W. and Narasimhan, T.N. (1989) Redox-controlled multiple-species reactive chemical transport, 1, Model development, Water Resour. Res., 25, 869-882.

Manning, B.A. and Goldberg, S. (1996) Modeling competitive adsorption of arsenate with phosphate and moybdate on oxide minerals, Soil Sci. Soc. Amer., 60, 121-131.

Martell, A.E. and Smith, R.M. (1989) Critical Stability Constants, Vol. 6, Second Supplement, New York, Plenum, 604 pp.

Masterson, J.P., Stone, B.D., Walter, D.A., and Savoie, J. (1997) Hydrogeologic framework of western Cape Cod, Massachusetts, U.S. Geological Survey Hydrologic Investigations Atlas, HA 740, 1 plate.

Morris, D.A., and Johnson, A.J. (1967) Summary of hydrologic and physical properties of rock and soil materials as analyzed by the Hydrologic Laboratory of the U.S. Geological Survey, 1948-1960, U.S. Geological Survey Professional Paper, 1839-D, 42 pp.

Nowack, B. and Sigg, L. (1996) Adsorption of EDTA and metal-EDTA complexes on goethite, J. Colloid Interface Sci., 177, 106-121.

Oldale, R.N. (1969) Seismic investigations on Cape Cod, Martha's Vineyard, and Nantucket, Massachusetts, and a topographic map of the basement surface from Cape Cod Bay to the Islands, U.S. Geological Survey Professional Paper, 650-B, B122-B127.

Parkhurst, D. L. (1995) User's guide to PHREEQC: A computer program for speciation, reaction-path, advective-transport, and inverse geochemical calculations, U.S. Geological Survey Water- Resources Investigation Report, 95-4227, 143 pp.

Perlmutter, N.M. and Lieber, M. (1970) Dispersal of plating wastes and sewage contamination in ground water and surface water, South Farmingdale-Massapequa area, Nassau County, New York, U.S. Geological Survey Water Supply Paper, 1879-G, 67 pp.

Rea, B.A., Kent, D.B., Anderson, L.C.D., Davis, J.A., and LeBlanc, D.R. (1996) The transport of inorganic contaminants in a sewage plume in the Cape Cod aquifer, Massachusetts, *in* Morganwalp, D.W. and Aronson, D.A., Eds., U.S. Geological Survey Toxic Substances Hydrology Program—Proceedings of the technical meeting, Colorado Springs, Colorado, September 20-24, 1993; U.S. Geological Survey Water-Resources Investigations Report, 94-4015, 191-198.

Rea, B.A., Kent, D.B., LeBlanc, D.R., and Davis, J.A. (1991) Mobility of zinc in a sewage-contaminated aquifer, Cape Cod, Massachusetts, *in* Mallard, G.E. and Aronson, D.A., Eds., U.S.Geological Survey Toxic Substances Hydrology Program—Proceedings of the technical meeting, Monterey, California, March 11-15, 1991, U.S. Geological Survey Water-Resources Investigations Report, 91-4034, 88-95.

Roberts, P.V., Goltz, M.N., and Mackay, D.M. (1986) A natural gradient experiment on solute transport in a sand aquifer, 3. Retardation estimates on mass balances for organic solutes, Water Resour. Res., 22(13), 2047-2058.

Rubin, J. (1990) Solute transport with multisegment, equilibrium-controlled reactions: A feed forward simulation method, Water Resour. Res., 26(9), 2029-2055.

Savoie, J., and LeBlanc, D.R., Eds., (1998) Water-quality data and methods of analysis for samples collected near a plume of sewage-contaminated ground water, Ashumet Valley, Cape Cod, Massachusetts, 1993-94, U.S. Geological Survey Water-Resources Investigations Report 97-4269, 208 pp.

Smith, R.M. and Martell, A.E. (1989) Critical Stability Constants, 6, Second Supplement, New York, Plenum, 643 pp.

Stollenwerk, K.G. (1995) Modeling the effects of variable groundwater chemistry on adsorption of molybdate, Water Resour. Res., 31(2), 347-357.

Stollenwerk, K.G. (1998) Molybdate transport in a chemically complex aquifer: Field measurements compared with solute-transport model predictions, Water Resour. Res., 34(10), 2727-2740.

Vaccaro, R.F., Kallio, P.E., Ketchum, B.H., Kerfoot, W.B., Mann, A., Deese, P.L., Palmer, C., Dennett, M.R., Bowker, P.C., Corwin, N., and Manganini, S.J., (1979) Wastewater renovation and retrieval on Cape Cod, U.S. Environmental Protection Agency, EPA-600/2-79-176, 174 pp.

Waite, T.D., Davis, J.A., Payne, T.E., Waychunas, G.A., and Xu, N. (1994) Uranium(VI) adsorption to ferrihydrite: Application of a surface complexation model, Geochim. Cosmochim. Acta, 58, 5465-5478.

Wood, W.W., Kraemer, T.F., and Hearn, P.P. Jr. (1990) Intragranular diffusion: An important mechanism influencing solute transport in clastic aquifers, Science, 147, 1569-1572.

Yeh, G.T. and Tripathi, V.S. (1989) A critical evaluation of recent developments of hydrogeochemical transport models of reactive multichemical components, Water Resour. Res., 25(1), 93-108.

Yeh, G.T. and Tripathi, V.S. (1991) A model for simulating transport of reactive multispecies components: Model development and demonstration, Water Resour. Res., 27(12), 3075-3094.

Tables

Table 1. Description of the Injectate and Injection Statistics

Constituent	*Reagent*	*Concentration*	*Concentration/MDL**
pH	-----	5.6	-----
Br^-	KBr	3.43 mM	1143
$EDTA^{4-}$	Na_4EDTA	1.112 mM	139
CrO_4^{2-}	$K_2Cr_2O_7$	0.506 mM (as Cr)	2663
Cu	$CuCl_2 \cdot 6H_2O$	0.266 mM	4222
Ni	$NiCl_2 \cdot 6H_2O$	0.256 mM	502
Pb	$Pb(NO_3)_2 \cdot 6H_2O$	0.248 mM	517
Zn	$ZnCl_2 \cdot 6H_2O$	0.266 mM	1773

Volume	9884 L
Altitude of Injection ports	13.17, 12.18, 11.18 m
Rate of Injection	1.02 L/min/port
Duration of Test	449 days (Day 0 = April 21, 1993)

***MDL = Method Detection Limit**

Table 2. Data from an Injection MLS and Three MLS 1.4 to 2 m from the Injection Center One Day after Injection

Part A: Tracers

MLS name and			*All concentrations are in micromolar*								
sample port altitude, m	*Br, mM*	*pH*	*Cr*	*Cu-total*	*Cu-EDTA*	*Ni-total*	*Ni-EDTA*	*Pb-total*	*Pb-EDTA*	*Zn-total*	*Zn-EDTA*
23B15- injection MLS											
13.82	0.209	5.43	0.78	0.65	0.74	0.94	<LOD	<LOD	<LOD	1.75	0.70
13.51	3.309	5.33	482.6	266.3	264.1	263.4	269.1	243.7	248.7	251.2	250.7
13.22	3.346	5.59	201.0	109.4	C	107.6	C	<LOD	<LOD	106.8	265.9
12.97	3.383	5.45	502.7	264.2	266.3	264.8	268.2	246.3	253.0	265.8	264.9
12.72	2.409	5.20	282.3	157.7	164.4	163.9	173.9	134.4	145.2	178.6	177.1
12.46	3.325	5.61	410.7	222.5	C	216.8	C	210.2	C	222.7	C
12.21	3.317	5.71	510.7	267.2	268.6	264.8	271.2	253.4	260.2	271.1	275.5
11.91	3.255	5.52	498.6	271.3	265.5	263.5	261.8	254.1	248.6	274.9	272.7
11.5	2.857	5.63	395.9	219.6	216.0	214.7	219.3	195.1	196.1	241.1	240.7
11.2	3.352	5.68	500.4	272.6	268.8	262.8	270.7	257.9	259.2	272.5	276.9
10.59	3.300	5.73	473.6	262.1	261.5	260.3	265.6	245.1	251.9	266.7	268.6
10.2	0.011	6.39	2.90	1.41	1.00	1.39	0.96	1.04	<LOD	1.13	0.75
9.8	0.192	n/s	28.4	15.0	16.8	14.1	15.9	12.4	14.5	13.6	15.7
9.3	0.057	n/s	9.47	5.16	4.69	4.94	4.51	4.40	4.18	4.84	4.32
8.7	0.298	n/s	43.3	23.9	24.8	22.5	23.9	21.0	22.0	22.5	23.8
2413A- 2 m downgradient (south) from injection center											
13.51	<LOD	5.70	<LOD	<LOD	<LOD	<LOD	<LOD	<LOD	<LOD	<LOD	<LOD
13.2	2.752	5.04	295.7	195.2	184.2	194.8	185.7	167.6	158.1	187.0	163.4
12.9	2.897	5.12	307.0	188.5	200.1	195.4	208.3	160.0	171.6	200.9	199.1
12.59	0.065	5.74	1.24	<LOD	<LOD	<LOD	<LOD	<LOD	<LOD	1.90	1.21
12.29	1.559	5.43	111.8	58.4	60.2	65.2	68.2	38.6	39.6	104.8	100.6
11.98	1.570	5.57	189.2	99.5	104.8	104.3	106.9	79.5	82.0	147.5	140.0
11.68	<LOD	6.07	<LOD	<LOD	<LOD	<LOD	<LOD	<LOD	<LOD	2.27	<LOD
11.38	<LOD	6.09	<LOD	<LOD	<LOD	<LOD	<LOD	<LOD	<LOD	2.33	<LOD
11.07	<LOD	6.30	34.1	21.9	25.4	25.4	29.6	13.3	15.9	47.1	50.1
10.61	<LOD	6.17	<LOD	0.14	0.14	<LOD	<LOD	<LOD	<LOD	<LOD	<LOD
10.15	<LOD	n/s	<LOD	0.18	0.25	<LOD	<LOD	<LOD	<LOD	<LOD	<LOD
2312- 2 m east of injection center											
12.12	0.011	5.81	1.11	1.33	0.81	0.63	0.68	<LOD	<LOD	2.81	1.35
11.87	0.146	5.91	15.43	8.75	8.31	8.75	8.62	3.35	3.44	18.76	15.66
11.61	<LOD	6.01	<LOD	0.42	<LOD	<LOD	<LOD	<LOD	<LOD	2.74	<LOD
11.37	<LOD	6.02	<LOD	0.33	<LOD	<LOD	<LOD	<LOD	<LOD	2.85	<LOD
2313- 1.4 m north east of injection center											
12.12	0.843	5.78	104.5	56.9	63.0	54.6	60.9	43.5	48.2	74.1	78.4
11.86	0.010	6.06	1.34	0.77	1.04	0.71	0.85	0.57	0.85	2.71	1.21
11.61	<LOD	6.12	0.46	0.40	0.31	<LOD	<LOD	<LOD	<LOD	2.63	0.46
11.37	<LOD	6.15	<LOD	0.22	<LOD	<LOD	<LOD	<LOD	<LOD	2.63	<LOD
11.11	0.048	6.14	7.42	4.18	<LOD	4.13	<LOD	2.64	<LOD	7.33	<LOD
10.86	<LOD	6.16	<LOD	<LOD	<LOD	<LOD	<LOD	<LOD	<LOD	0.76	<LOD

NOTES: No EDTA measurements were made on these samples.
n/s indicates no sample collected
<LOD indicates values were below detection
C indicates probable contamination.

Table 2. Data from an Injection MLS and Three MLS 1.4 to 2 m from the Injection Center One Day after Injection

Part B: Additional sediment reactive constituents.

MLS name and sample port altitude, m	*All concentrations are in micromolar* *Al-total*	*Al-EDTA*	*Fe-total*	*Fe-EDTA*	*Mn-total*
23B15- injection MLS					
13.82	<LOD	<LOD	1.03	1.09	<LOD
13.51	49.48	53.97	12.43	12.80	<LOD
13.22	17.14	C	3.15	C	<LOD
12.97	40.91	45.89	8.23	8.45	0.72
12.72	20.15	26.03	14.30	15.07	2.14
12.46	25.56	C	5.56	C	1.36
12.21	29.54	32.32	6.07	6.12	2.35
11.91	25.56	23.57	5.39	5.45	2.32
11.5	14.74	18.85	8.55	9.15	9.97
11.2	25.45	31.02	6.87	7.06	2.95
10.59	10.97	<LOD	11.54	11.72	32.96
10.2	<LOD	<LOD	0.49	0.38	4.05
9.8	<LOD	<LOD	1.61	1.53	2.33
9.3	<LOD	<LOD	0.76	0.68	4.03
8.7	<LOD	<LOD	2.07	1.90	2.48
2413A- 2 m downgradient (south) from injection center					
13.51	<LOD	<LOD	<LOD	<LOD	<LOD
13.2	40.2	37.1	16.2	15.7	1.75
12.9	27.7	30.6	10.1	10.1	1.46
12.59	<LOD	<LOD	<LOD	<LOD	<LOD
12.29	5.75	4.91	3.22	3.29	0.32
11.98	8.40	9.89	2.78	2.77	0.42
11.68	<LOD	<LOD	<LOD	<LOD	1.00
11.38	<LOD	<LOD	<LOD	<LOD	4.18
11.07	<LOD	<LOD	2.17	2.48	11.35
10.61	<LOD	<LOD	<LOD	<LOD	6.77
10.15	<LOD	<LOD	<LOD	<LOD	6.17
2312- 2 m east of injection center					
12.12	<LOD	<LOD	<LOD	<LOD	<LOD
11.87	<LOD	<LOD	0.38	0.38	<LOD
11.61	<LOD	<LOD	<LOD	<LOD	1.93
11.37	<LOD	<LOD	<LOD	<LOD	4.29
2313- 1.4 m north east of injection center					
12.12	2.62	2.37	2.09	2.25	<LOD
11.86	<LOD	<LOD	<LOD	<LOD	<LOD
11.61	<LOD	<LOD	<LOD	<LOD	1.39
11.37	<LOD	<LOD	<LOD	<LOD	3.86
11.11	<LOD	<LOD	0.34	<LOD	6.36
10.86	<LOD	<LOD	0.17	<LOD	7.62

NOTES: No EDTA measurements were made on these samples.
n/s indicates no sample collected
<LOD indicates values were below detection
C indicates probable contamination.

Table 3. Sample Types and Chemical Data Collected

Sample Type	*Treatment*	*Electrode measurements*	*Absorbance Spectrophotometry*	*ICP-AES*
Anion (60 mL)	R	pH, Br	Br, Cr(VI), EDTA	---
Cation (20-30 mL)	F/A/R	---	---	total dissolved metals
Metal speciation (20 mL)	F/X/A/R	---	---	EDTA-metal complexes

R= refrigerated at 4 ^{o}C; **F**= filtered inline to <0.45 microns;
A= acidified with 6 N HCl; **X**= passed through chelex-100 resin

Table 4. Summary of Analytical Methods

Constituent	*Analytical error*	*Method Limit of Detection*	*Reference*
Br^-	±5-10%	3 µM	Kent et al., 1994
pH	±0.15 pH units	----	Estimated, this study
O_2(aq)-probe	±10%	30 µM	Kent et al., 1994
O_2(aq)-Chemet	±20%	0.03 µM	Kent et al., 1994
EDTA	±7 µM	2 µM [1] 8 µM [2]	Estimated, this study
Cr(VI)	±5%	0.3 µM	Kent et al., 1994
Dissolved Metals, ICP-AES			
Cr	±5%	0.19 µM	Estimated, this study[3]
Cu	±5%	0.063 µM	Estimated, this study[3]
Ni	±5%	0.51 µM	Estimated, this study[3]
Pb	±5%	0.48 µM	Estimated, this study[3]
Zn	±5%	0.15 µM	Estimated, this study[3]
Fe	±5%	0.14 µM	Estimated, this study[3]
Al	±7%	1.9 µM	Estimated, this study[3]

[1] Refers to groundwater collected from the pristine zone of the aquifer.
[2] Refers to groundwater collected from the sewage-contaminated zone of the aquifer.
[3] Relative standard deviation of values measured at ten times the reported MDL. Values <10x MDL have significantly higher %RSD values (±10-25%).

Table 5. Br Data Summary for Breakthrough MLS: BT1 and BT2

BT#1, 37 m downgradient				BT#2, 52 m downgradient			
Altitude	***Δt***	***Avg. T(i)***	α_L	***Altitude***	***Δt***	***Avg. T(i)***	α_L
m	***days***	***days***	***m***	***m***	***days***	***days***	***m***
13.51	--	--	--	13.65	--	--	--
13.21	--	--	--	13.14	np	--	--
12.90	19.5	61.2	0.38	12.63	24.8	78.3	0.48
12.60	10.3	56.7	0.11	12.13	15.0	96.9	0.11
12.14	11.7	67.4	0.10	11.62	34.6	111	0.45
11.68	17.7	82.1	0.16	11.11	18.5	98.2	0.17
11.23	30.4	77.7	0.51	10.60	17.7	95.5	0.17
10.77	16.6	67.9	0.20	10.10	19.2	114	0.14
10.30	8.5	71.0	0.05	9.59	19.8	125	0.12
9.85	28.7	85.5	0.48	9.08	22.7	134	0.14
9.39	23.8	94.2	0.23	8.58	20.5	126	0.13
8.93	11.9	97.7	0.06	8.07	10.0	110	0.04
8.47	11.1	93.1	0.05	7.56	4.2	99.1	0.01
8.02	8.3	90.0	0.03	7.05	--	--	--
7.56	5.6	79.1	0.02	6.54	--	--	--

np = no peak, but bromide was detectable.

Figures

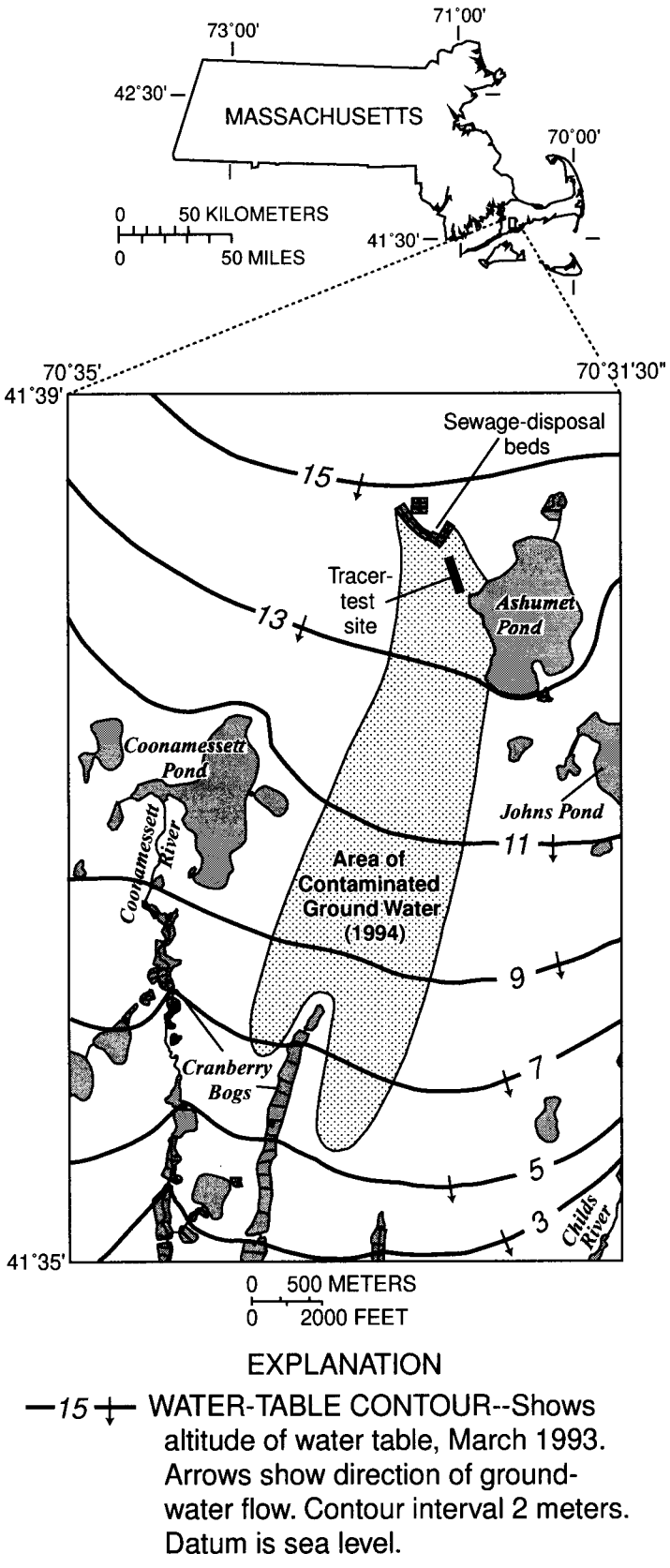

Figure 1. Location of tracer-test site, area of sewage-contaminated groundwater, and general water-table contours, western Cape Cod, Massachusetts.

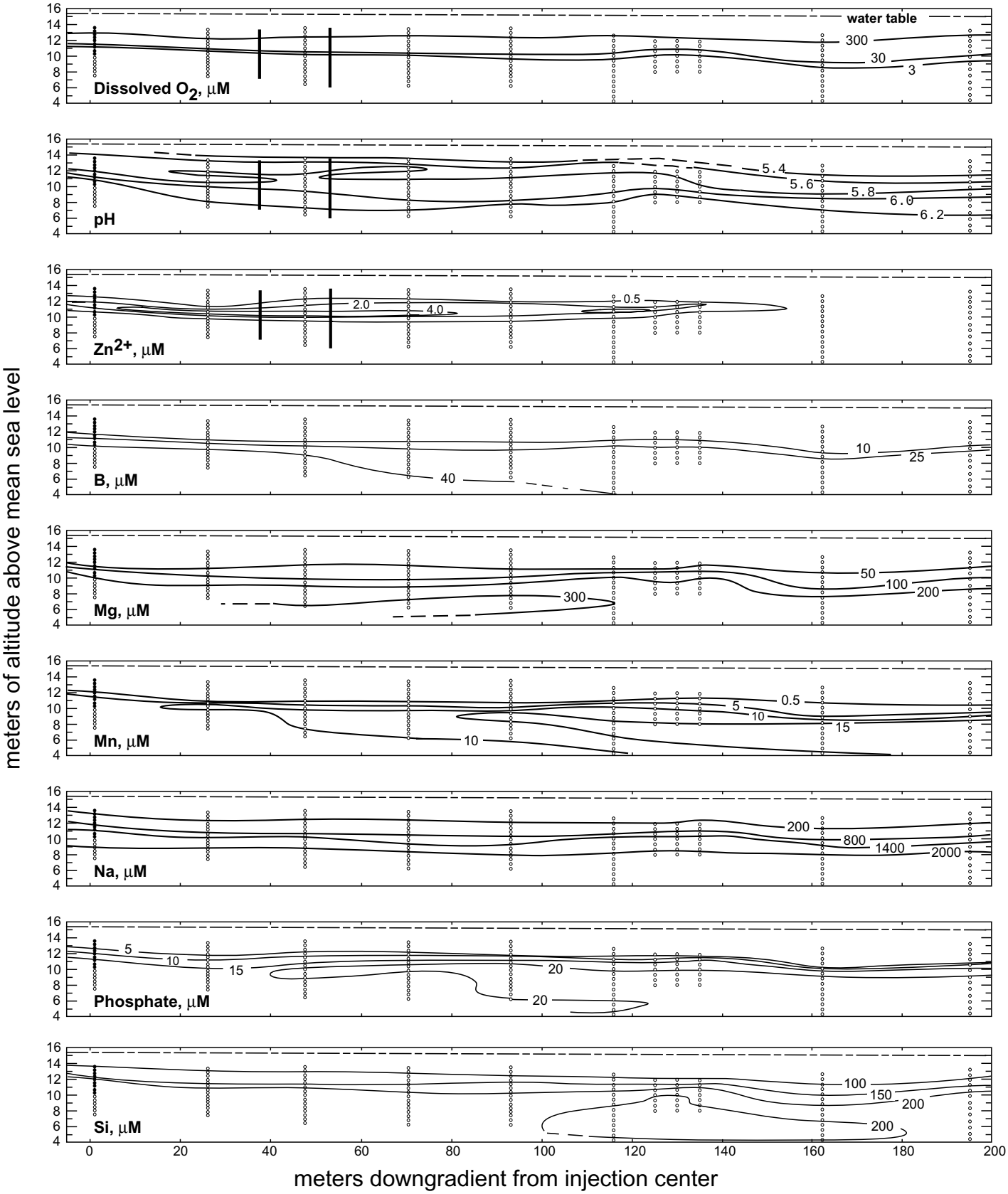

Figure 2. Longitudinal cross sections showing the distributions of various water quality parameters in the aquifer in April 1993 just prior to the field experiment. The area shown is downgradient from the injection location. The small circles indicate the locations where groundwater was collected. The filled small circles at the extreme left indicate the vertical spreading of the tracer cloud just after the injection. Solid bars on the panels with data for DO, pH, and dissolved Zn show the locations of the two MLS used to collect data for constructing breakthrough curves. Location of the transect is shown in Figure 3.

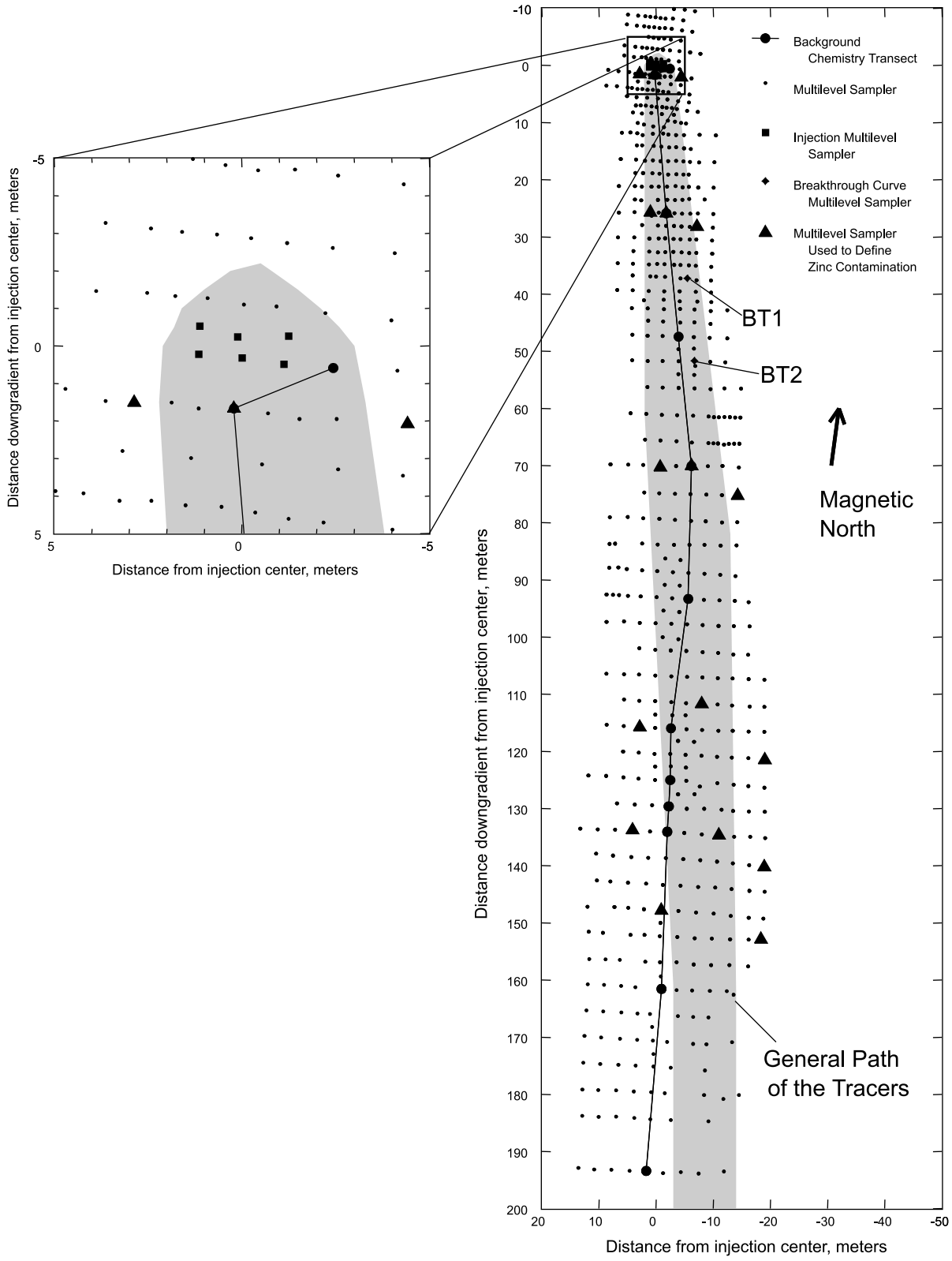

Figure 3. Locations of the general path of tracers, the multilevel samplers (MLS) available for sampling during the tracer test, the six injection MLS, the two breakthrough curve MLS, and the MLS used to construct background chemistry transects and to define the extent of zinc contamination.

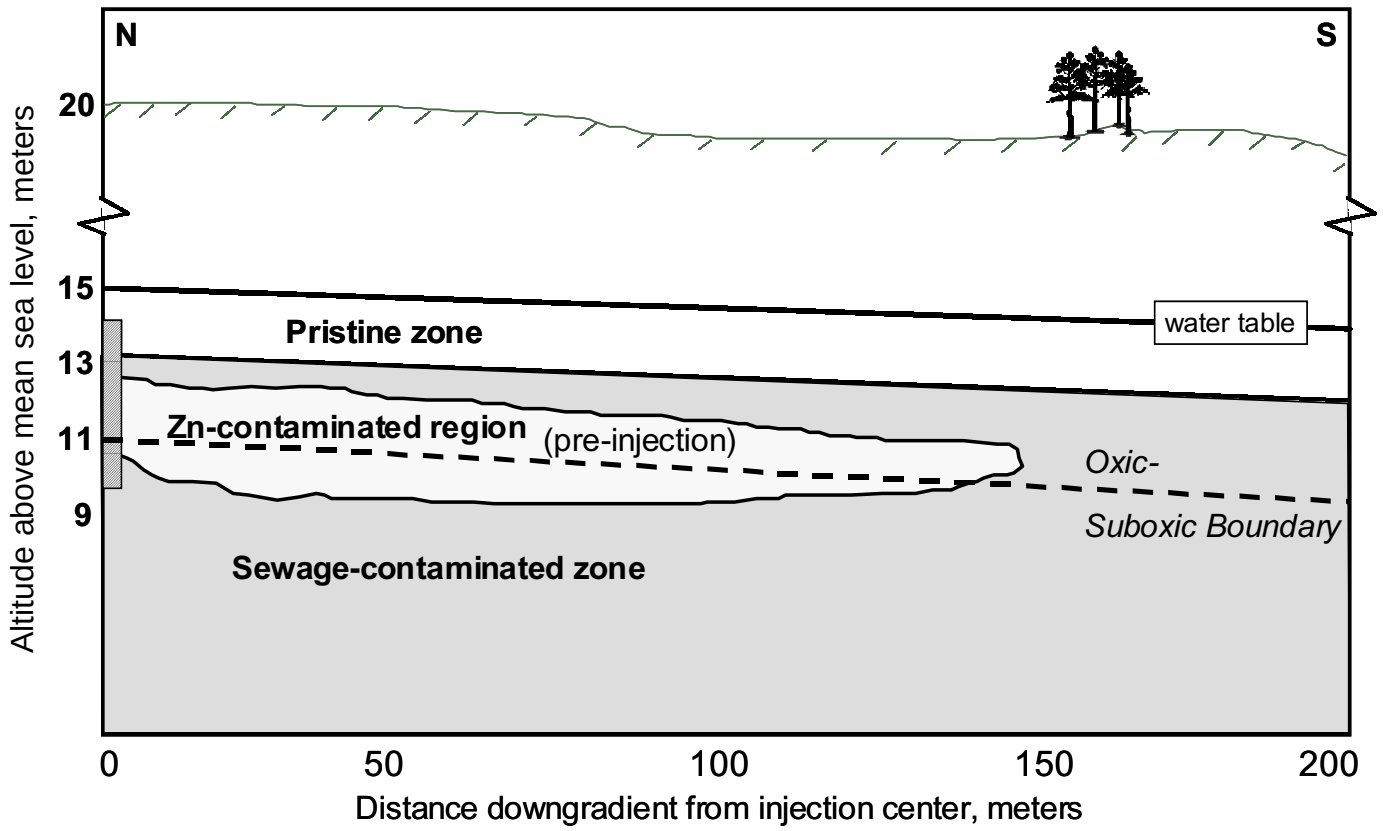

Figure 4. Generalized longitudinal cross section showing the spatial relationships between the different aquifer zones defined in the study. The hatched rectangle at the extreme left indicates the vertical range covered by the injection relative to the various geochemical conditions.

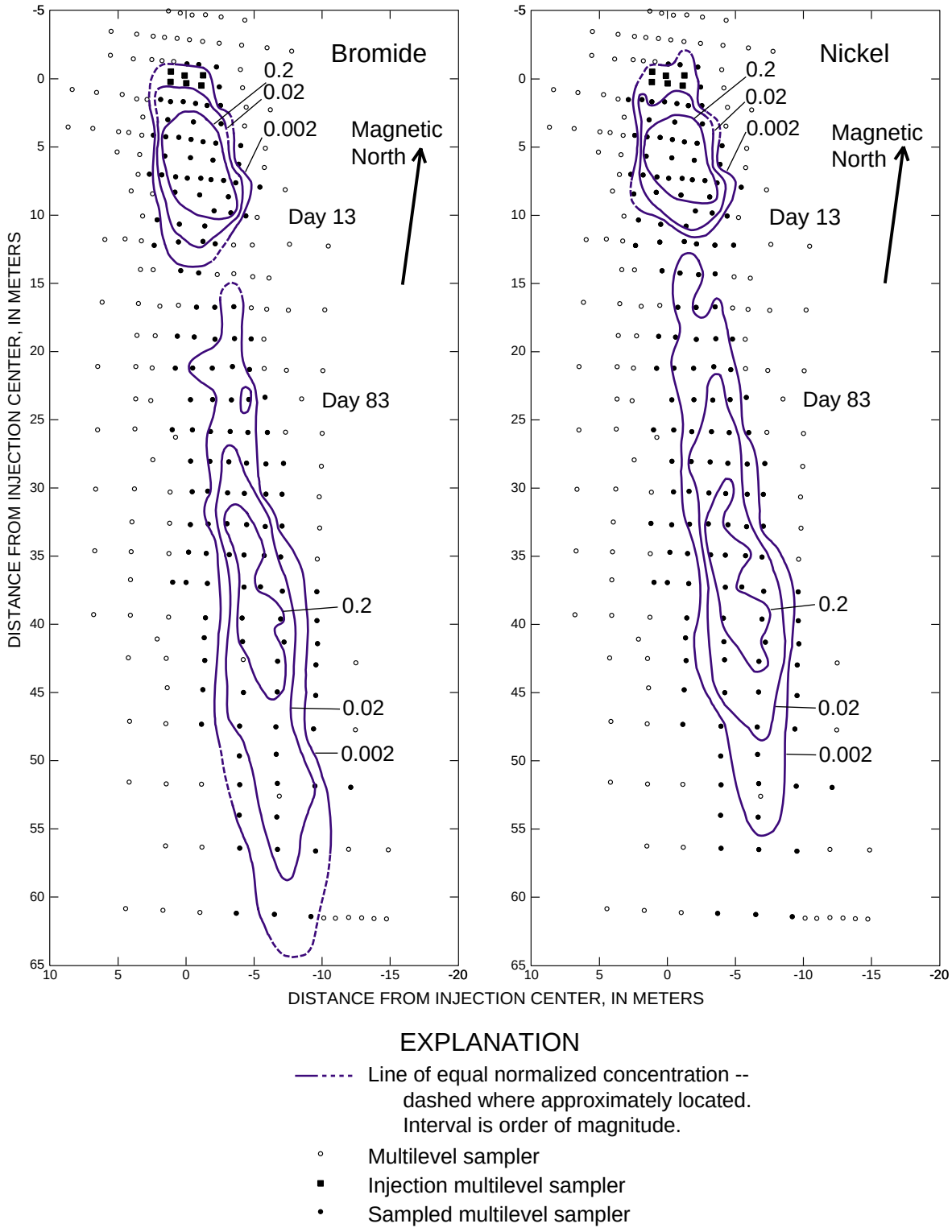

Figure 5. Mapped distributions of the maximum Br and Ni concentrations of each MLS for the synoptic samplings at 13 and 83 days after the injection. Concentrations normalized by dividing by the injection concentrations.

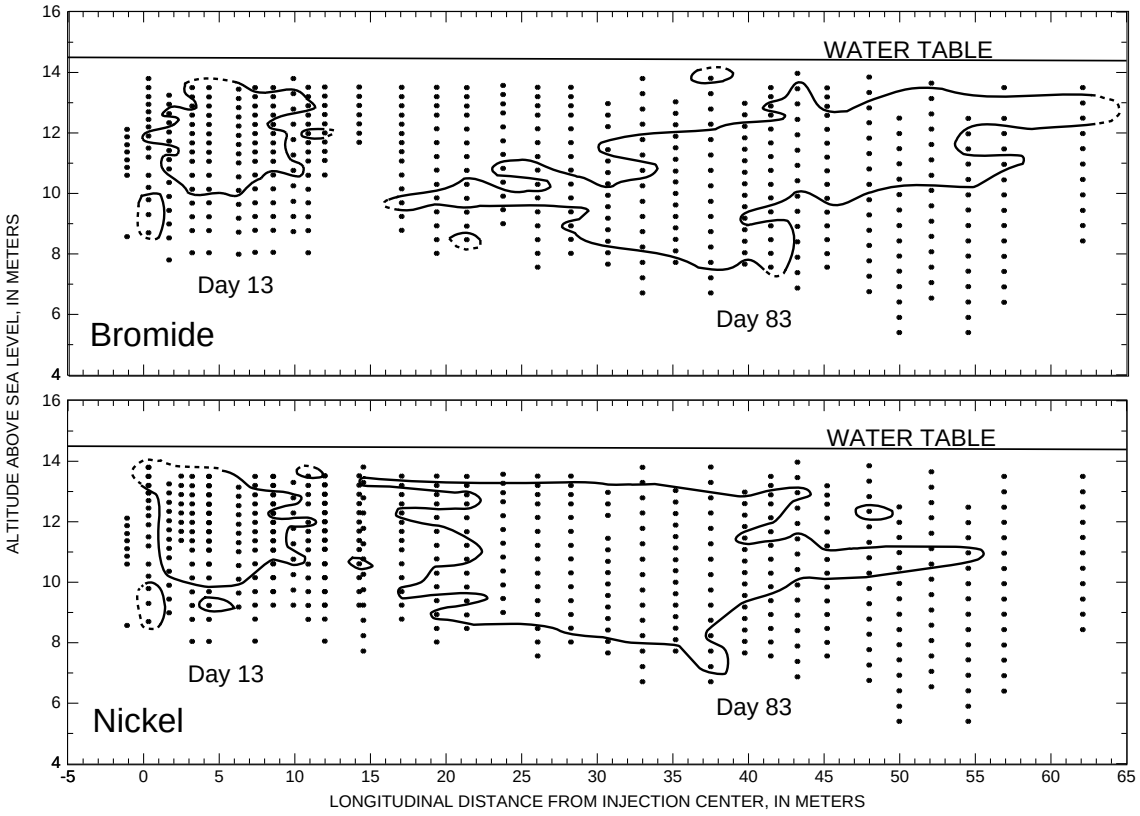

Figure 6. Longitudinal and vertical extents of Br and Ni concentrations observed 13 and 83 days after injection. Section aligned along the mean direction of transport. Extents of tracers marked by the 0.002 concentration contours, normalized by the injection concentrations.

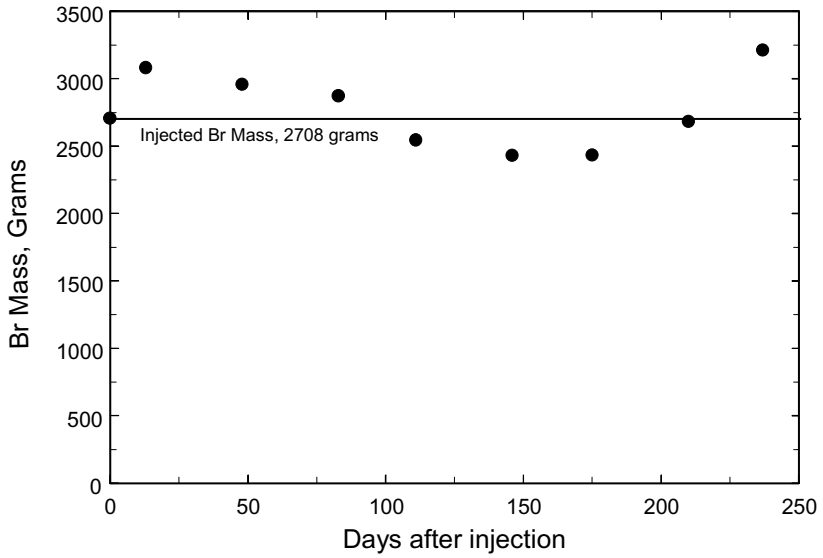

Figure 7. Calculated Br mass (zeroth moment) for each synoptic sampling.

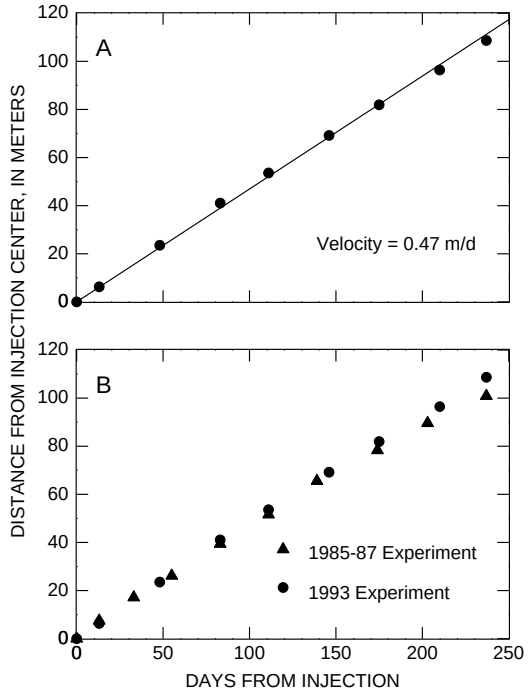

Figure 8. (A) Calculated distance from the center of injection to the center of mass of Br (first moment) for each synoptic sampling. (B) Comparison of distances calculated in this (1993) and earlier (1985-87; Garabedian et al, 1991) experiments.

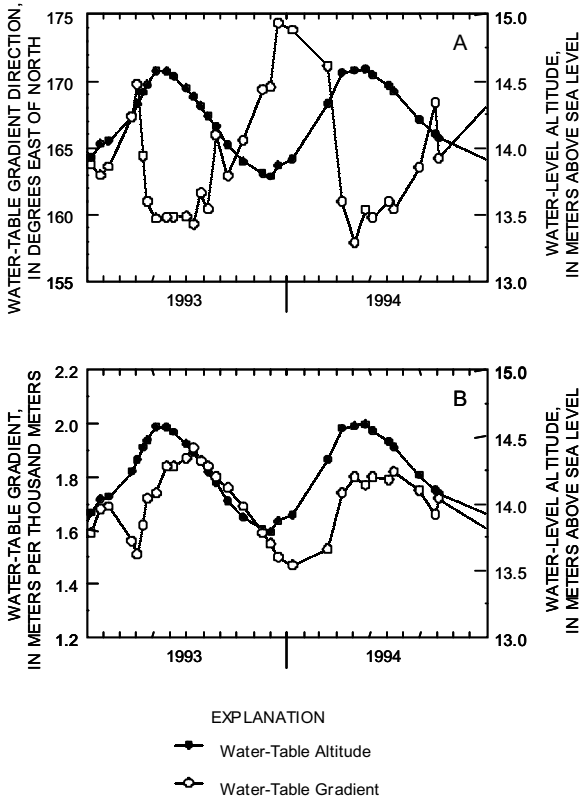

Figure 9. Water-table altitude measured in observation well FSW 343-36 (1.17 m, -46.66 m) and water-table gradient direction and magnitude calculated from water-table altitudes measured in three observation wells (FSW 343-36, FSW 382-32 (66.57 m, 127.58 m), and FSW 414-36 (-87.17 m, 98.69 m)) at tracer-test site for 1993-94. The spatial coordinates of the three wells (given in parenthesis: x, y) are in the same coordinate system used in all figures with the system centered on the tracer-test injection and aligned along the mean direction of transport observed in the earlier large-scale tracer test (LeBlanc et al., 1991).

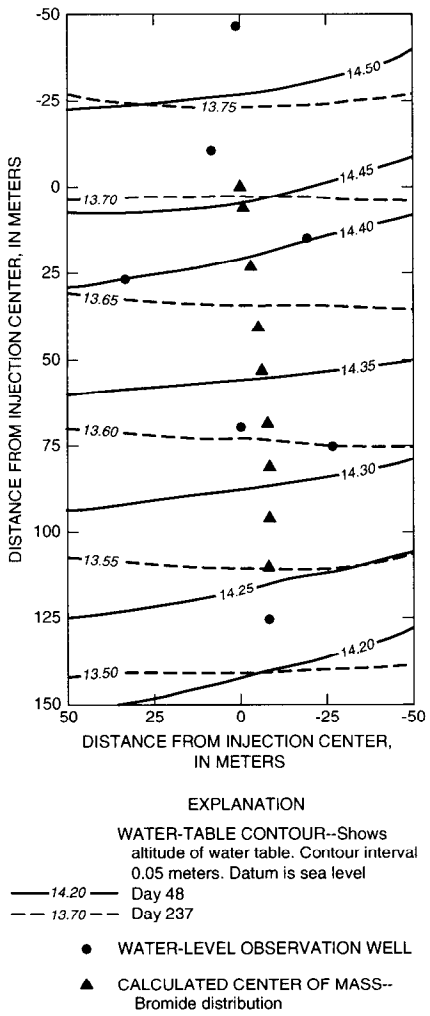

Figure 10. Calculated location of the center of mass of Br (first moment) for each synoptic sampling. Water-table contours shown for 48 (solid lines) and 237 (dashed lines) days after injection. Locations of only 7 of the 25 observation wells from which water-level data was collected are shown. Others are located outside the mapped area.

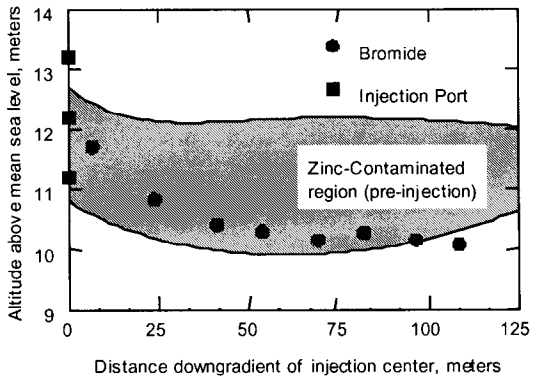

Figure 11. Calculated altitude of the center of mass of Br (first moment) for each synoptic sampling is shown as a function of the distance transported downgradient from the injection and relative to the Zn-contaminated region.

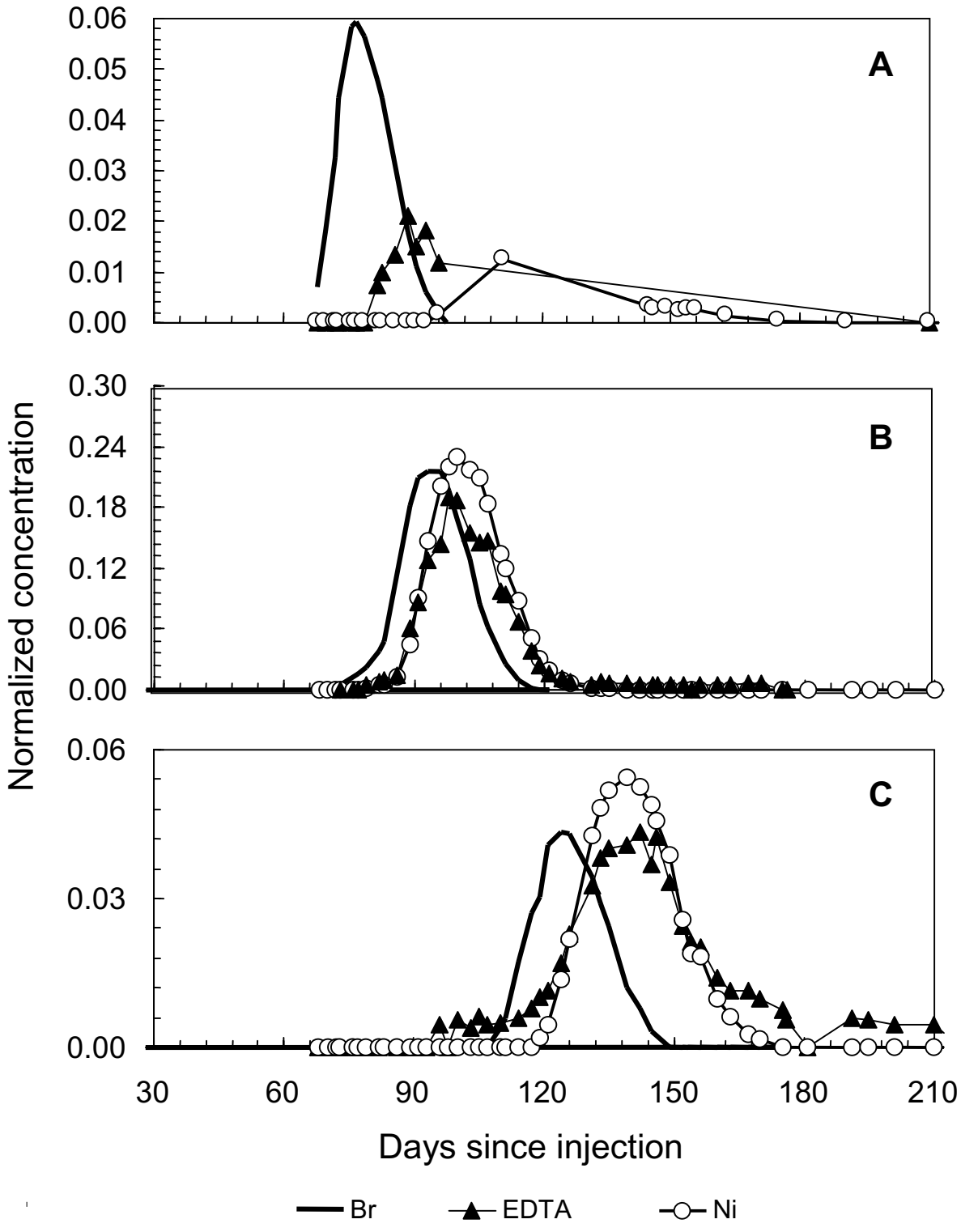

Figure 12. Typical pattern of breakthrough for Br, Ni, and EDTA. Concentrations normalized by dividing by the injection concentrations. (A) Pristine zone, 37 meters downgradient, 12.9 m altitude; (B) Zn-contaminated region, 52 meters downgradient, 10.6 meters altitude; (C) suboxic zone, 52 meters downgradient, 8.58 meters altitude.

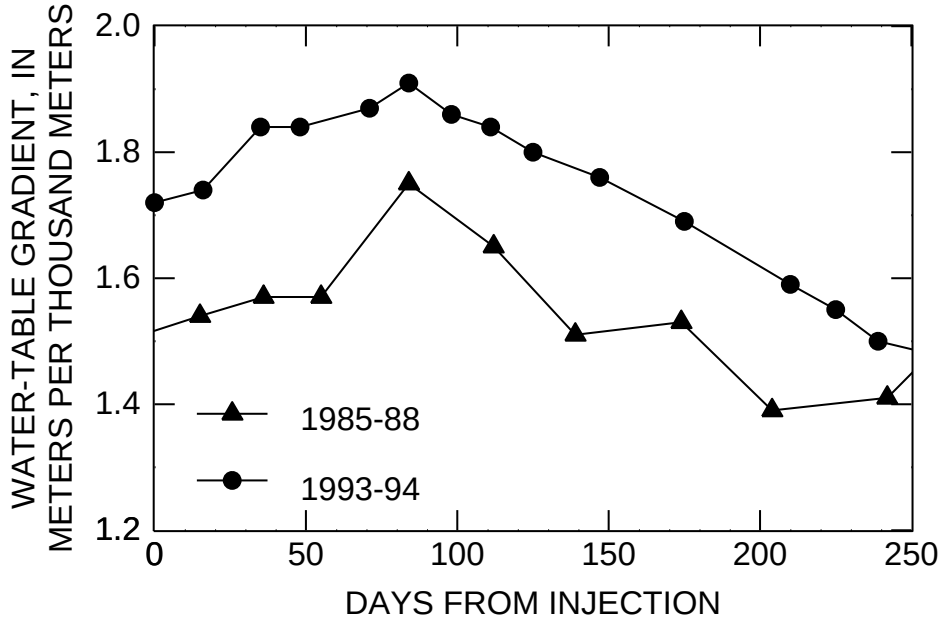

Figure 13. Comparison of water-table gradients calculated for this (1993) and earlier (1985-88; LeBlanc et al., 1991) experiments.

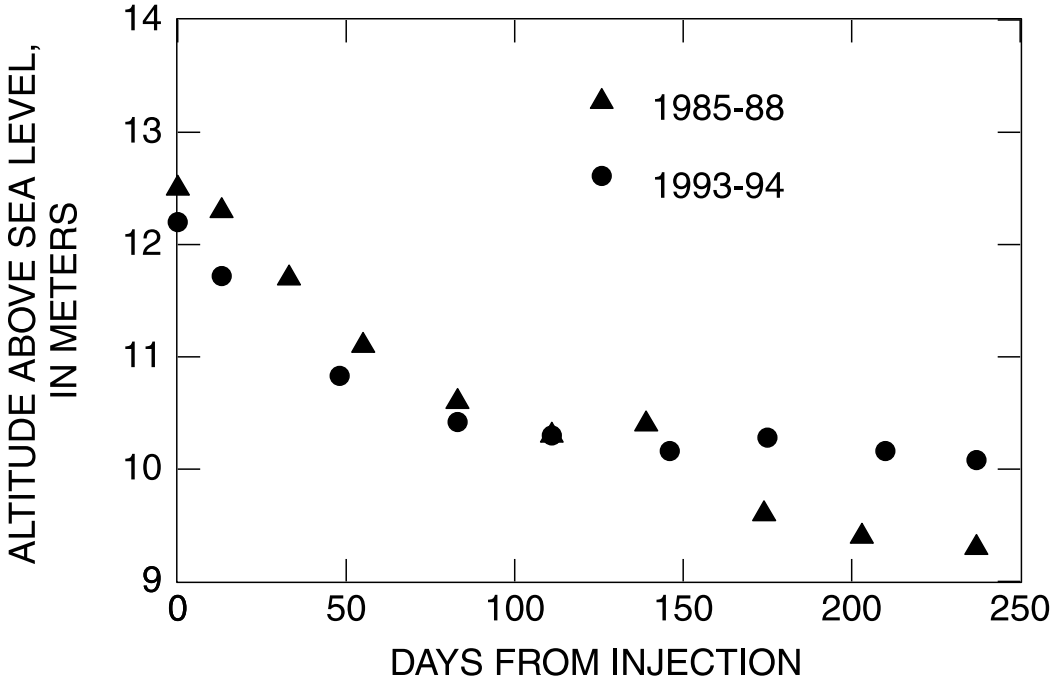

Figure 14. Comparison of calculated altitude of center of mass of Br for each synoptic sampling for this (1993) and earlier (1985-88; Garabedian et al., 1991) experiments.

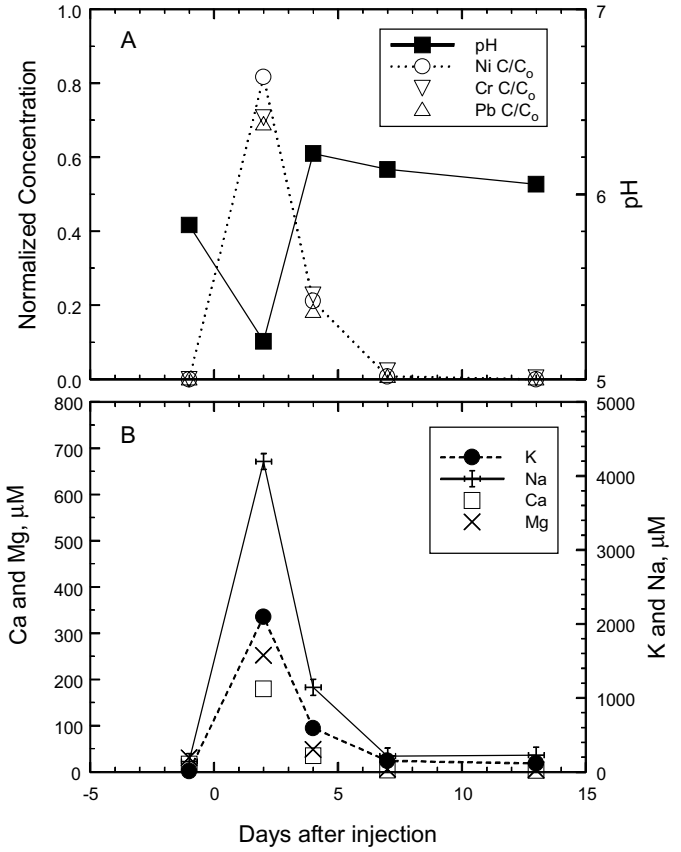

Figure 15. Concentration versus time plots at a sampling port in the pristine zone (13.0 m above mean sea level) at a distance 1.7 m downgradient from the center of the array of injection MLS. Location of MLS (2414A) is shown in Figure 3 (filled triangle closest to the array of injection MLS). (A) Normalized concentrations of Ni, Cr, and Pb (scale on left-hand side) and pH values (scale on right-hand side). (B) Concentrations of Ca and Mg (scale on the left-hand side) and K and Na (scale on the right-hand side).

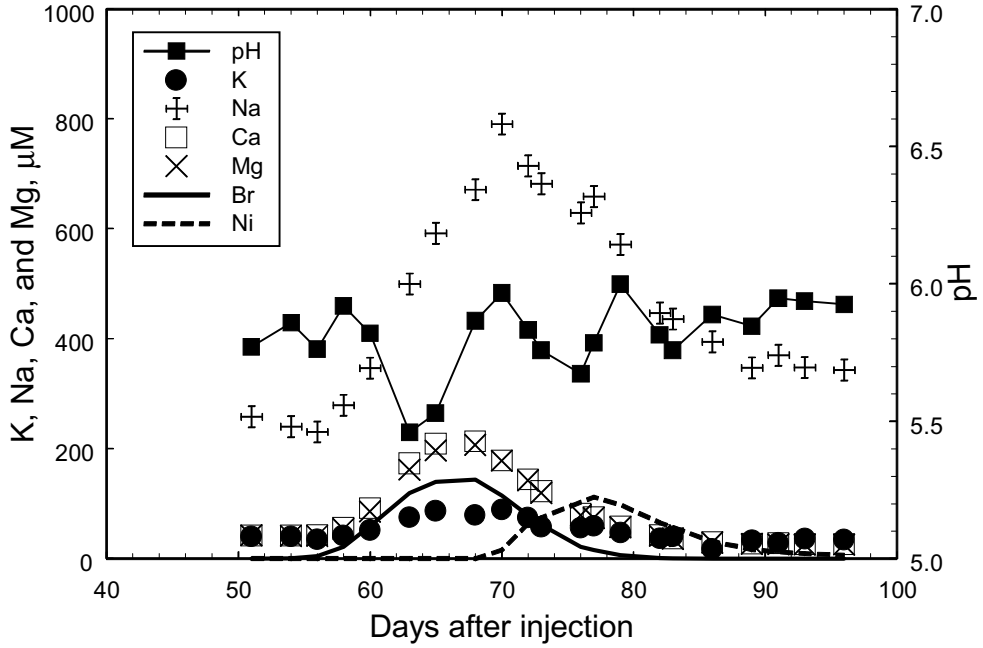

Figure 16. Breakthrough curves (BT1, Fig. 3, 37 m downgradient) from the pristine zone (12.1 m above mean sea level) for K, Na, Ca, Mg (scale on left-hand side) and for pH (scale on right-hand side). Also shown are breakthrough curves for Br and Ni, in arbitrary concentration units, in order to illustrate the delay between the pH fluctuation and the breakthrough of reactive tracers.

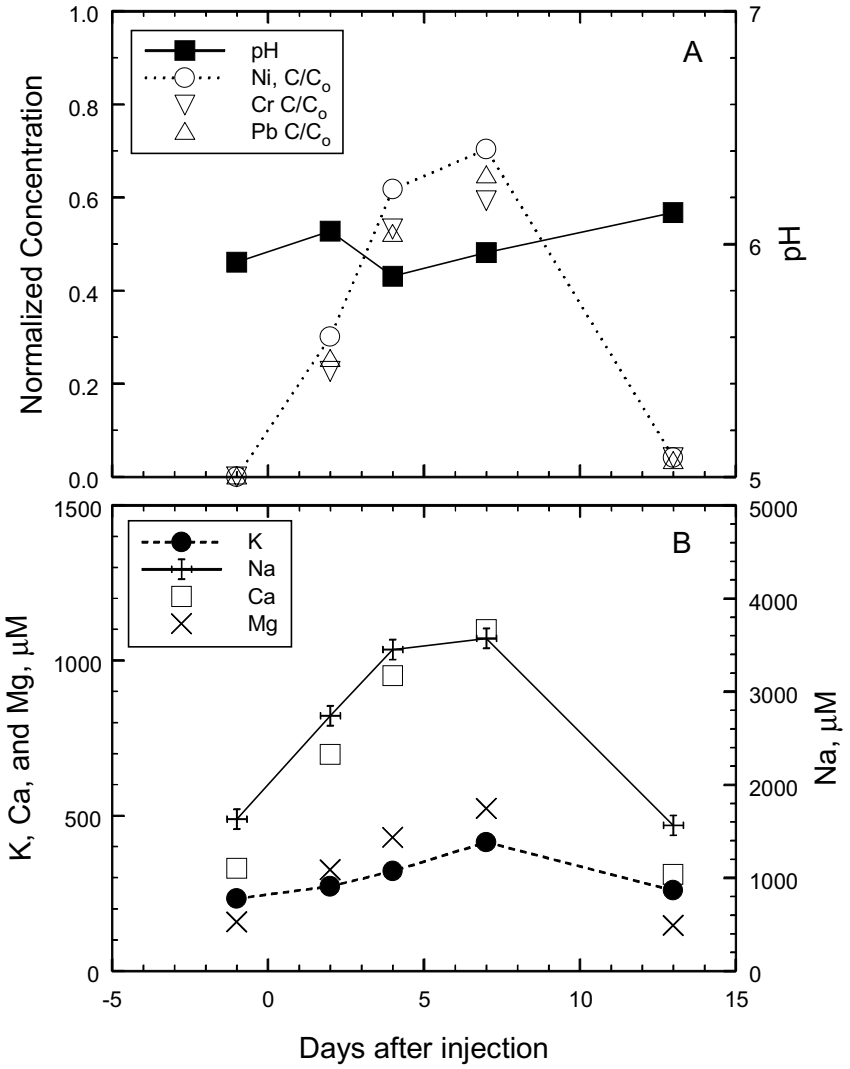

Figure 17. Concentration versus time plots at a sampling port in the transition zone (10.8 m above mean sea level) at a distance 1.7 m downgradient from the center of the array of injection MLS. Location of MLS (2414A) is shown in Figure 3 (filled triangle closest to the array of injection MLS). (A) Normalized concentrations of Ni, Cr, and Pb (scale on left-hand side) and pH (scale on right-hand side). (B) Concentrations of K, Ca, and Mg (scale on the left-hand side) and Na (scale on the right-hand side).

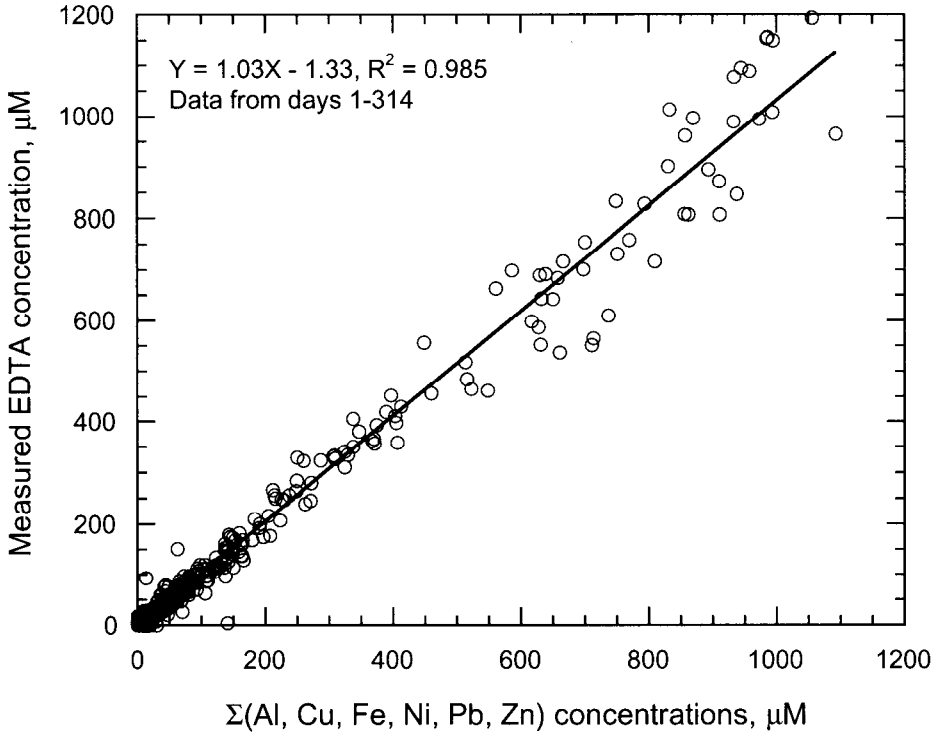

Figure 18. Correlation between the sum of the concentrations of dissolved Cu, Ni, Zn, Pb, Al, and Fe, and measured EDTA concentrations. Data are from metal speciation samples in the synoptic and breakthrough curve samplings. Samples were collected at several elevations of BT1, BT2, and along a longitudinal transect of MLS through the center of the tracer clouds during the synoptic samplings.

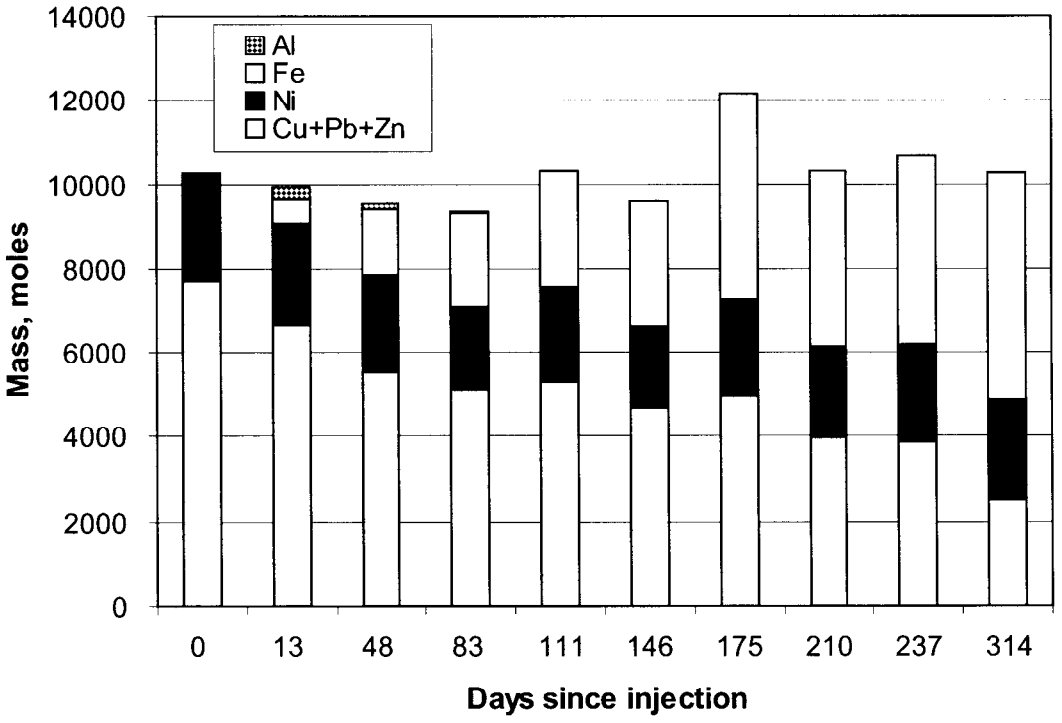

Figure 19. Mass distribution of metals complexed with EDTA in the tracer cloud as a function of time after injection. The total height of the bar for each sampling represents an estimate of the mass of EDTA being transported.

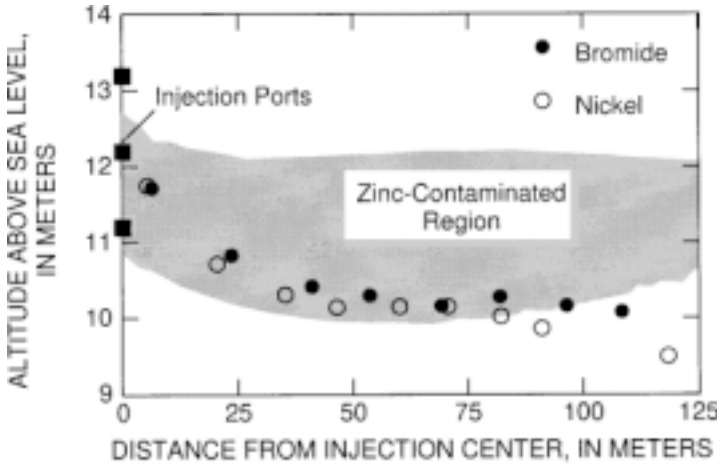

Figure 20. Calculated altitudes of the centers of mass of Br and Ni (first moments) for each synoptic sampling relative to the horizontal distance traveled. Extent of Zn-contaminated region defined by 0.5 μM concentration contour shown in Figure 3.

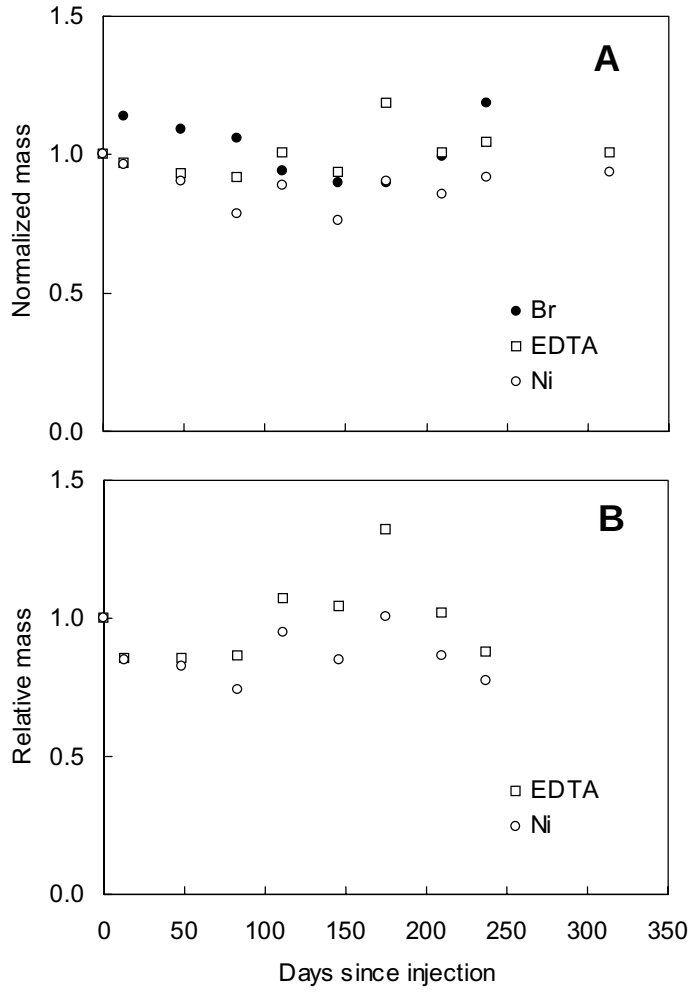

Figure 21. (A) Calculated Br, EDTA, and Ni masses (zeroth moments) for each synoptic sampling normalized by the total mass of injected tracer. (B) Relative mass of Ni and EDTA calculated by dividing the normalized mass by the normalized Br mass for each synoptic sampling. The EDTA mass was increasingly overestimated with time, because the sum includes an unknown mass of Zn^{2+} present in the Zn-contaminated region.

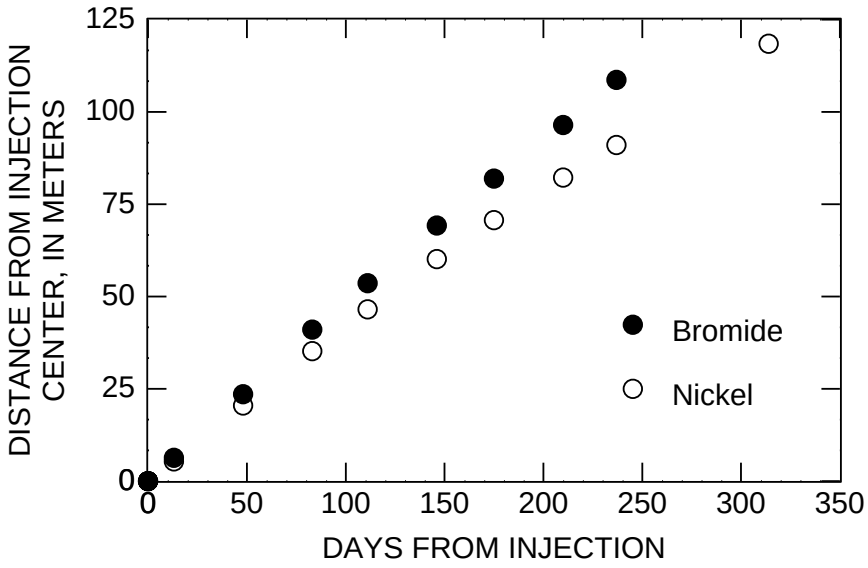

Figure 22. Calculated distances from the center of injection to the center of mass of Br and Ni (first moments) for each synoptic sampling.

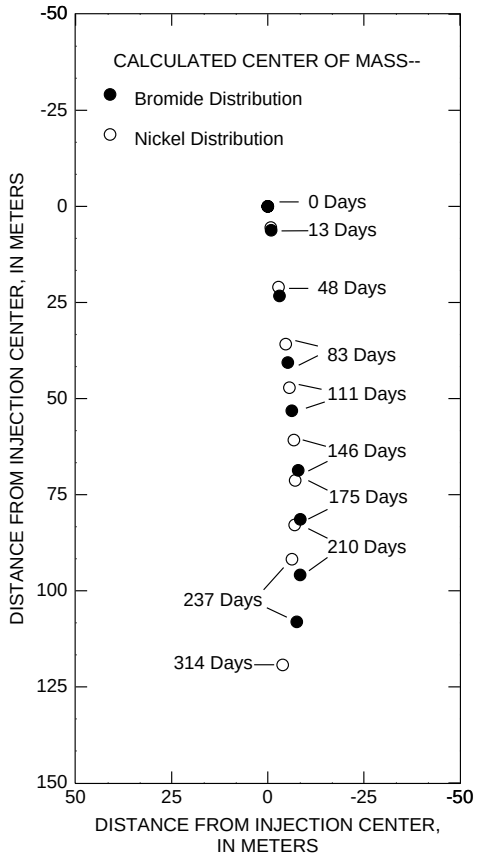

Figure 23. Calculated location of the centers of mass of Br and Ni (first moments) for each synoptic sampling.

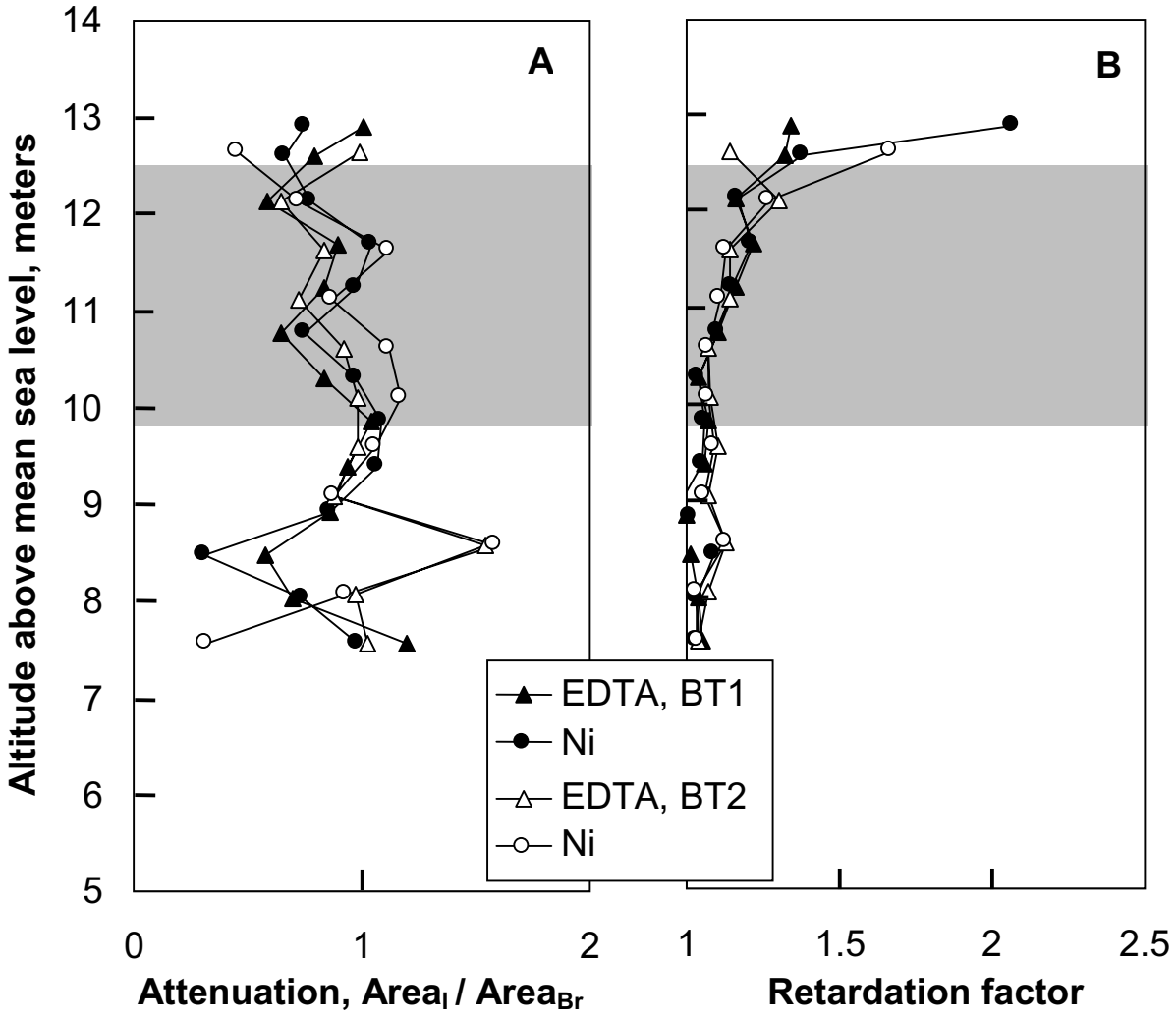

Figure 24. Transport parameters for EDTA and Ni at BT1 and BT2. The shaded area indicates the sampling ports in the Zn-contaminated region. (A) Attenuation of EDTA and Ni relative to the mass of Br transported. (B) Retardation of EDTA and Ni relative to Br.